

# 10 Complexation and Protein Binding

## Chapter Objectives

At the conclusion of this chapter the student should be able to:

1. Define the three classes of complexes (coordination compounds) and identify pharmaceutically relevant examples.
2. Describe chelates, their physical properties, and what differentiates them from organic molecular complexes.
3. Describe the types of forces that hold together organic molecular complexes and give examples.
4. Describe the forces involved in polymer–drug complexes used for drug delivery and situations where reversible or irreversible complexes may be advantageous.
5. Discuss the uses and give examples of cyclodextrins in pharmaceutical applications.
6. Determine the stoichiometric ratio and stability constant for complex formation.
7. Describe the methods of analysis of complexes and their strengths and weaknesses.
8. Discuss the ways that protein binding can influence drug action.
9. Describe the equilibrium dialysis and ultrafiltration methods for determining protein binding.
10. Understand the factors affecting complexation and protein binding.
11. Understand the thermodynamic basis for the stability of complexes.

Complexes or coordination compounds, according to the classic definition, result from a donor–acceptor mechanism or Lewis acid–base reaction between two or more different chemical constituents. Any nonmetallic atom or ion, whether free or contained in a neutral molecule or in an ionic compound, that can donate an electron pair can serve as the donor. The acceptor, or constituent that accepts a share in the pair of electrons, is frequently a metallic ion, although it can be a neutral atom. Complexes can be divided broadly into two classes depending on whether the acceptor component is a metal ion or an organic molecule; these are classified according to one possible arrangement in Table 10-1. A third class, the inclusion/occlusion compounds, involving the entrapment of one compound in the molecular framework of another, is also included in the table.

Intermolecular forces involved in the formation of complexes are the van der Waals forces of dispersion, dipolar, and induced dipolar types. Hydrogen bonding provides a significant force in some molecular complexes, and coordinate covalence is important in metal complexes. Charge transfer and hydrophobic interaction are introduced later in the chapter.

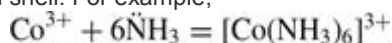
## Metal Complexes

A satisfactory understanding of metal ion complexation is based upon a familiarity with atomic structure and molecular forces, and the reader would do well to consult texts on inorganic and organic chemistry to study those sections dealing with electronic structure and hybridization before proceeding.

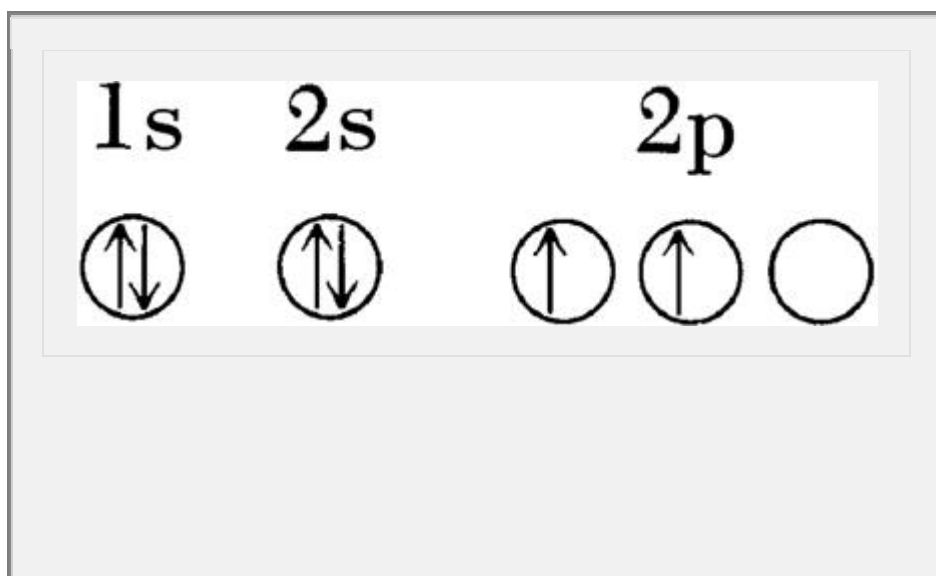
## Inorganic Complexes

The ammonia molecules in hexamminecobalt (III) chloride, as the compound  $[\text{Co}(\text{NH}_3)_6]^{3+} \text{Cl}_3^-$  is called, are known as the *ligands* and are said to be *coordinated* to the cobalt ion. The *coordination number* of the cobalt ion, or number of ammonia groups coordinated to the metal ions, is six. Other complex ions belonging to the inorganic group include  $[\text{Ag}(\text{NH}_3)_2]^+$ ,  $[\text{Fe}(\text{CN})_6]^{4-}$ , and  $[\text{Cr}(\text{H}_2\text{O})_6]^{3+}$ .

Each ligand donates a pair of electrons to form a coordinate covalent link between itself and the central ion having an incomplete electron shell. For example,



Hybridization plays an important part in coordination compounds in which sufficient bonding orbitals are not ordinarily available in the metal ion. The reader's understanding of hybridization will be refreshed by a brief review of the argument advanced for the quadrivalence of carbon. It will be recalled that the ground-state configuration of carbon is



This cannot be the bonding configuration of carbon, however, because it normally has four rather than two valence electrons. Pauling<sup>1</sup> suggested the possibility of *hybridization* to account for the quadrivalence. According to this mixing process, one of the 2s electrons is promoted to P.198

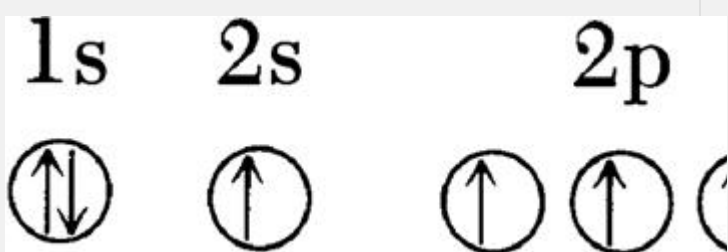
the available 2p orbital to yield four equivalent bonding orbitals:

**Table 10-1 Classification of Complexes\***

- I. Metal ion complexes
  - A. Inorganic type
  - B. Chelates
  - C. Olefin type
  - D. Aromatic type
    - 1. Pi ( $\pi$ ) complexes
    - 2. Sigma ( $\sigma$ ) complexes
    - 3. "Sandwich" compounds
- II. Organic molecular complexes
  - A. Quinhydrone type
  - B. Picric acid type
  - C. Caffeine and other drug complexes
  - D. Polymer type
- III. Inclusion/occlusion compounds
  - A. Channel lattice type
  - B. Layer type
  - C. Clathrates
  - D. Monomolecular type
  - E. Macromolecular type

\*This classification does not pretend to describe the mechanism or the type of chemical bonds involved in complexation. It is meant simply to separate

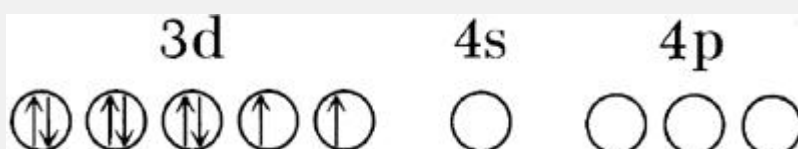
out the various types of complexes that are discussed in the literature. A highly systematized classification of electron donor–acceptor interactions is given by R. S. Mulliken, *J. Phys. Chem.* **56**, 801, 1952.



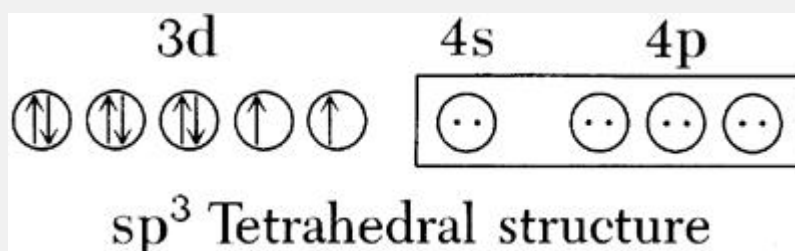
These are directed toward the corners of a tetrahedron, and the structure is known as an  $sp^3$  hybrid because it involves one s and three p orbitals. In a double bond, the carbon atom is considered to be  $sp^2$  hybridized, and the bonds are directed toward the corners of a triangle.

Orbitals other than the 2s and 2p orbitals can become involved in hybridization. The transition elements, such as iron, copper, nickel, cobalt, and zinc, seem to make use of their 3d, 4s, and 4p orbitals in forming hybrids. These hybrids account for the differing geometries often found for the complexes of the transition metal ions. Table 10-2 shows some compounds in which the central atom or metal ion is hybridized differently and the geometry that results.

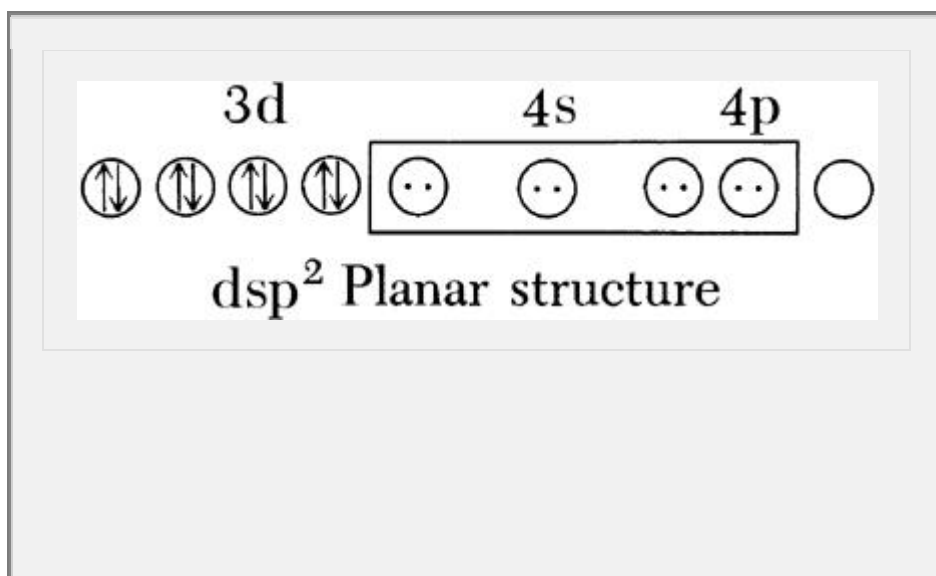
Ligands such as  $\text{H}_2\ddot{\text{O}}$ ,  $\text{H}_3\ddot{\text{N}}$ ,  $\text{C}\ddot{\text{N}}^-$ , or  $\text{C}\ddot{\text{I}}$  donate a pair of electrons in forming a complex with a metal ion, and the electron pair enters one of the unfilled orbitals on the metal ion. A useful but not inviolate rule to follow in estimating the type of hybridization in a metal ion complex is to select that complex in which the metal ion has its 3d levels filled or that can use the lower-energy 3d and 4s orbitals primarily in the hybridization. For example, the ground-state electronic configuration of  $\text{Ni}^{2+}$  can be given as



In combining with  $4\text{C}\ddot{\text{N}}^-$  ligands to form  $[\text{Ni}(\text{CN})_4]^{2-}$ , the electronic configuration of the nickel ion may become either

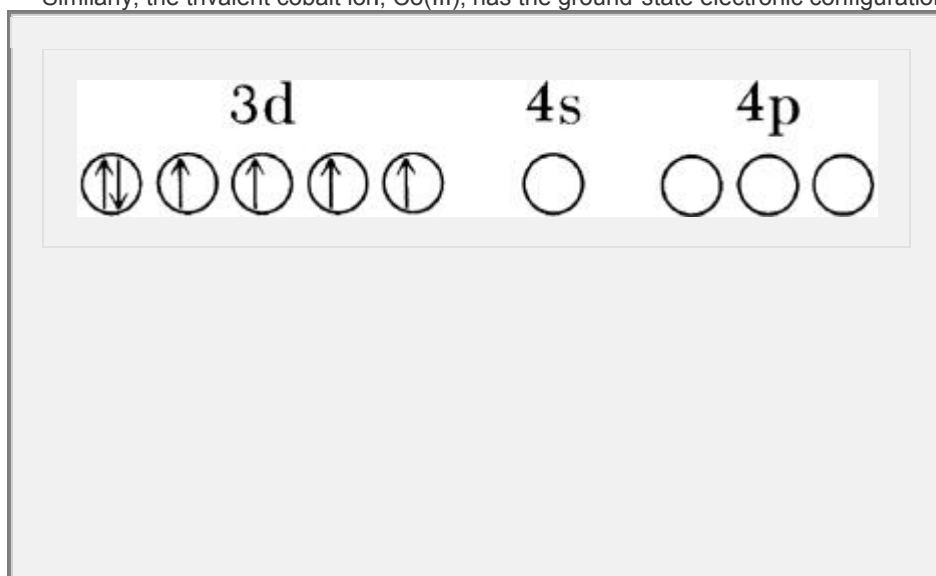


or

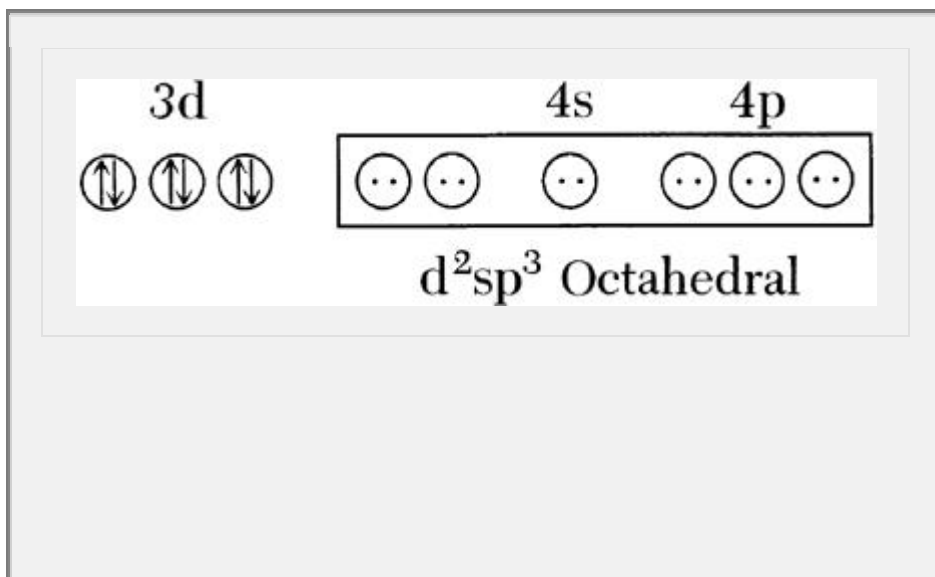


in which the electrons donated by the ligand are shown as dots. The  $dsp^2$  or square planar structure is predicted to be the complex formed because it uses the lower-energy 3d orbital. By the preparation and study of a number of complexes, Werner deduced many years ago that this is indeed the structure of the complex.

Similarly, the trivalent cobalt ion,  $Co(III)$ , has the ground-state electronic configuration

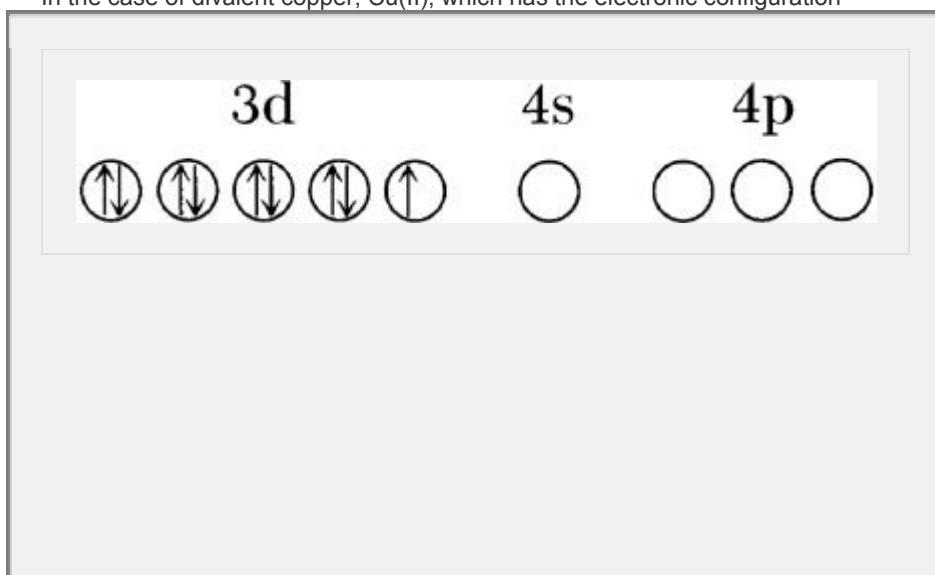


and one may inquire into the possible geometry of the complex  $[Co(NH_3)_6]^{3+}$ . The electronic configuration of the metal ion leading to filled 3d levels is

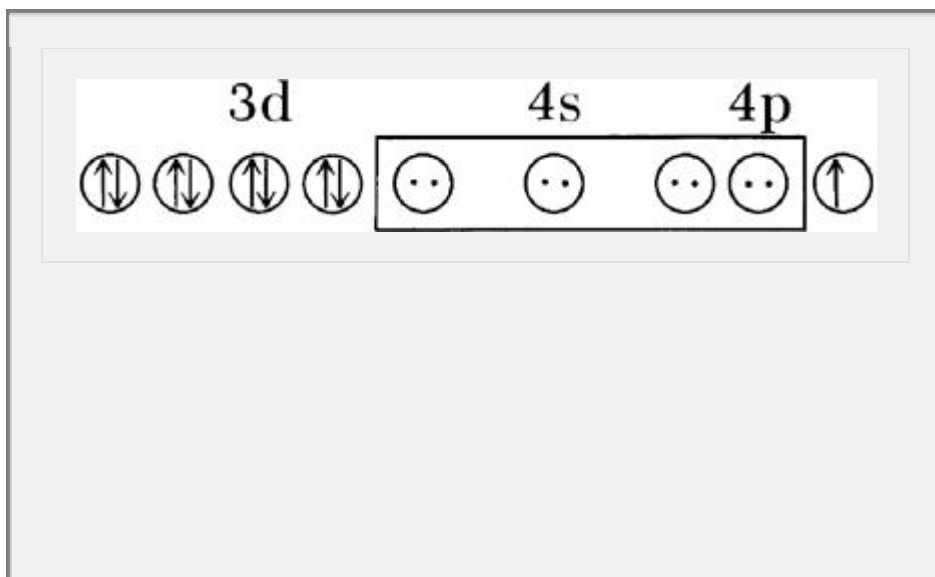


and thus the  $d^2sp^3$  or octahedral structure is predicted as the structure of this complex. Chelates (see following section) of octahedral structure can be resolved into optical isomers, and in an elegant study, Werner used this technique to prove that cobalt complexes are octahedral.

In the case of divalent copper,  $Cu(II)$ , which has the electronic configuration



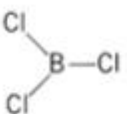
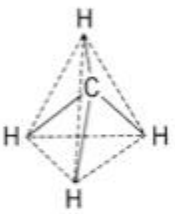
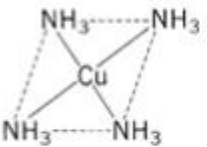
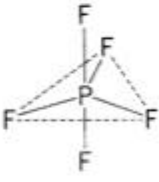
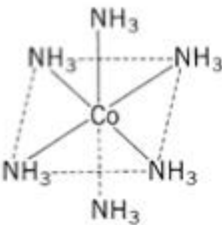
the formation of the complex  $[Cu(NH_3)_4]^{2+}$  requires the promotion of one d electron of  $Cu^{2+}$  to a 4p level to obtain a filled 3d configuration in the complexed metal ion, and a  $dsp^2$  or planar structure is obtained:



Although the energy required to elevate the d electron to the 4p level is considerable, the formation of a planar complex

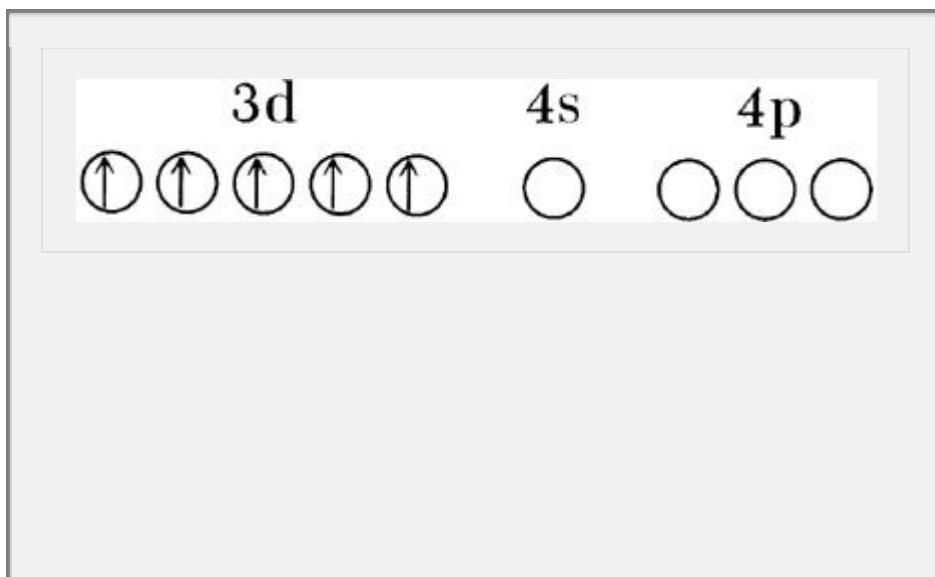
P.199

having the 3d levels filled entirely more than "pays" for the expended energy.

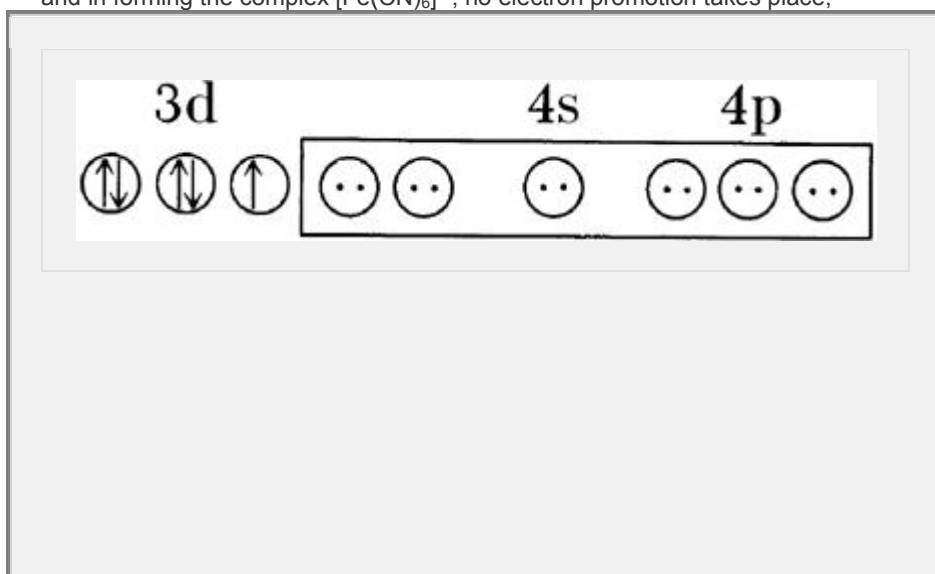
Coordination Number	Orbital Configuration	Bond Geometry	Example	
			Formula	Structure
2	$sp$	Linear	$O_2$	$O-O$
3	$sp^2$	Trigonal	$BCl_3$	
4	$sp^3$	Tetrahedral	$CH_4$	
4	$dsp^2$	Square planar	$Cu(NH_3)_4^{2+}$	
5	$dsp^3$	Bipyramidal	$PF_5$	
6	$d^2sp^3$	Octahedral	$Co(NH_3)_6^{3+}$	

**Table 10-2 Bond Types of Representative Compounds**

The metal ion  $Fe(III)$  has the ground-state configuration



and in forming the complex  $[\text{Fe}(\text{CN})_6]^{3-}$ , no electron promotion takes place,



because no stabilization is gained over that which the  $d^2sp^3$  configuration already possesses.

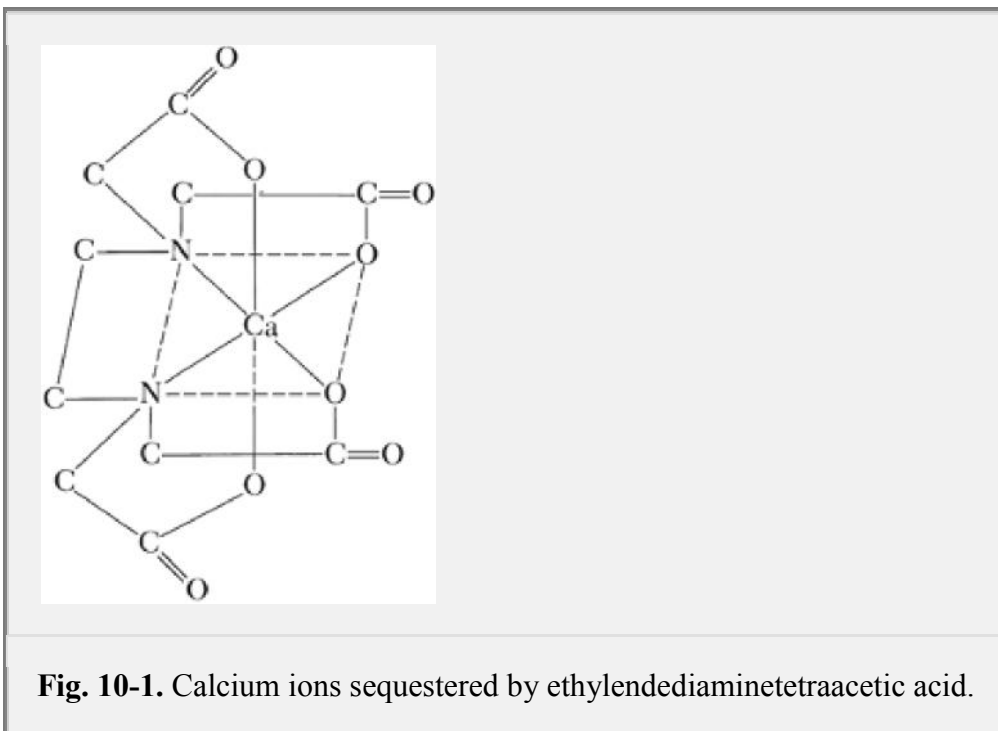
Compounds of this type, in which the ligands lie “above” a partially filled orbital, are termed *outer-sphere complexes*; when the ligands lie “below” a partially filled orbital, as in the previous example, the compound is termed an *inner-sphere complex*. The presence of unpaired electrons in a metal ion complex can be detected by *electron spin resonance spectroscopy*.

### **Chelates**

Chelation places stringent steric requirements on both metal and ligands. Ions such as Cu(II) and Ni(II), which form square planar complexes, and Fe(III) and Co(III), which form octahedral complexes, can exist in either of two geometric forms. As a consequence of this isomerism, only *cis-coordinated ligands*—ligands adjacent on a molecule—will be readily replaced by reaction with a chelating agent. Vitamin B<sub>12</sub> and the hemoproteins are incapable of reacting with chelating agents because their metal is already coordinated in such a way that only the *trans* coordination positions of the metal are available for complexation. In contrast, the metal ion in certain enzymes, such as alcohol dehydrogenase, which contains

P.200

zinc, can undergo chelation, suggesting that the metal is bound in such a way as to leave two *cis* positions available for chelation.



Chlorophyll and hemoglobin, two extremely important compounds, are naturally occurring chelates involved in the life processes of plants and animals. Albumin is the main carrier of various metal ions and small molecules in the blood serum. The amino-terminal portion of human serum albumin binds Cu(II) and Ni(II) with higher affinity than that of dog serum albumin. This fact partly explains why humans are less susceptible to copper poisoning than are dogs. The binding of copper to serum albumin is important because this metal is possibly involved in several pathologic conditions.<sup>3</sup> The synthetic chelating agent ethylenediaminetetraacetic acid (Fig. 10-1) has been used to tie up or *sequester* iron and copper ions so that they cannot catalyze the oxidative degradation of ascorbic acid in fruit juices and in drug preparations. In the process of sequestration, the chelating agent and metal ion form a water-soluble compound. Ethylenediaminetetraacetic acid is widely used to sequester and remove calcium ions from hard water.

**Key Concept**

**Chelates**

A substance containing two or more donor groups may combine with a metal to form a special type of complex known as a *chelate* (Greek: “kelos, claw”). Some of the bonds in a chelate may be ionic or of the primary covalent type, whereas others are coordinate covalent links. When the ligand provides one group for attachment to the central ion, the chelate is called *monodentate*. Pilocarpine behaves as a monodentate ligand toward Co(II), Ni(II), and Zn(II) to form chelates of pseudotetrahedral geometry.<sup>7</sup>

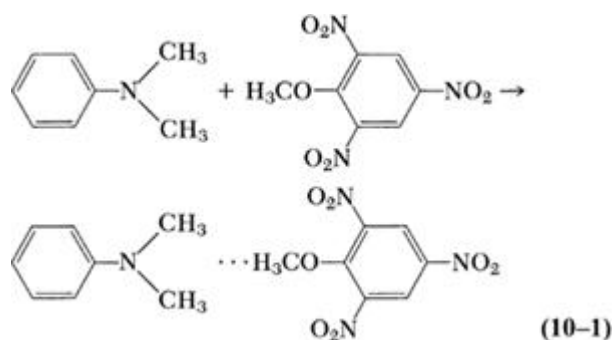
The donor atom of the ligand is the pyridine-type nitrogen of the imidazole ring of pilocarpine. Molecules with two and three donor groups are called *bidentate* and *tridentate*, respectively. Ethylenediaminetetraacetic acid has six points for attachment to the metal ion and is accordingly *hexadentate*; however, in some complexes, only four or five of the groups are coordinated.

Chelation can be applied to the assay of drugs. A calorimetric method for assaying procainamide in injectable solutions is based on the formation of a 1:1 complex of procainamide with cupric ion at pH 4 to 4.5. The complex absorbs visible radiation at a maximum wavelength of 380 nm.<sup>4</sup> The many uses to which metal complexes and chelating agents can be put are discussed by Martell and Calvin.<sup>5</sup>

## Organic Molecular Complexes

An organic coordination compound or molecular complex consists of constituents held together by weak forces of the donor–acceptor type or by hydrogen bonds.

The difference between complexation and the formation of organic compounds has been shown by Clapp. The compounds dimethylaniline and 2,4,6-trinitroanisole react in the cold to give a molecular complex:



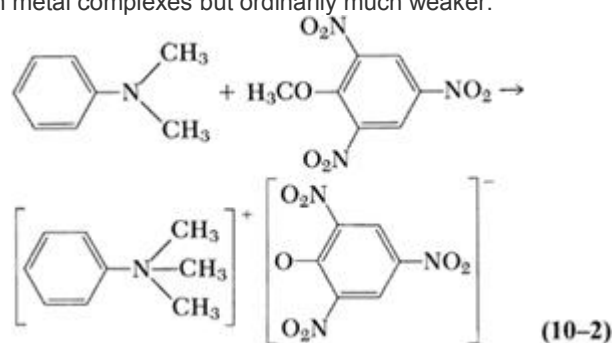
On the other hand, these two compounds react at an elevated temperature to yield a salt, the constituent molecules of which are held together by primary valence bonds:

The dotted line in the complex of equation (10-1) indicates that the two molecules are held together by a weak secondary valence force. It is not to be considered as a clearly defined bond but rather as an overall attraction between the two aromatic molecules.

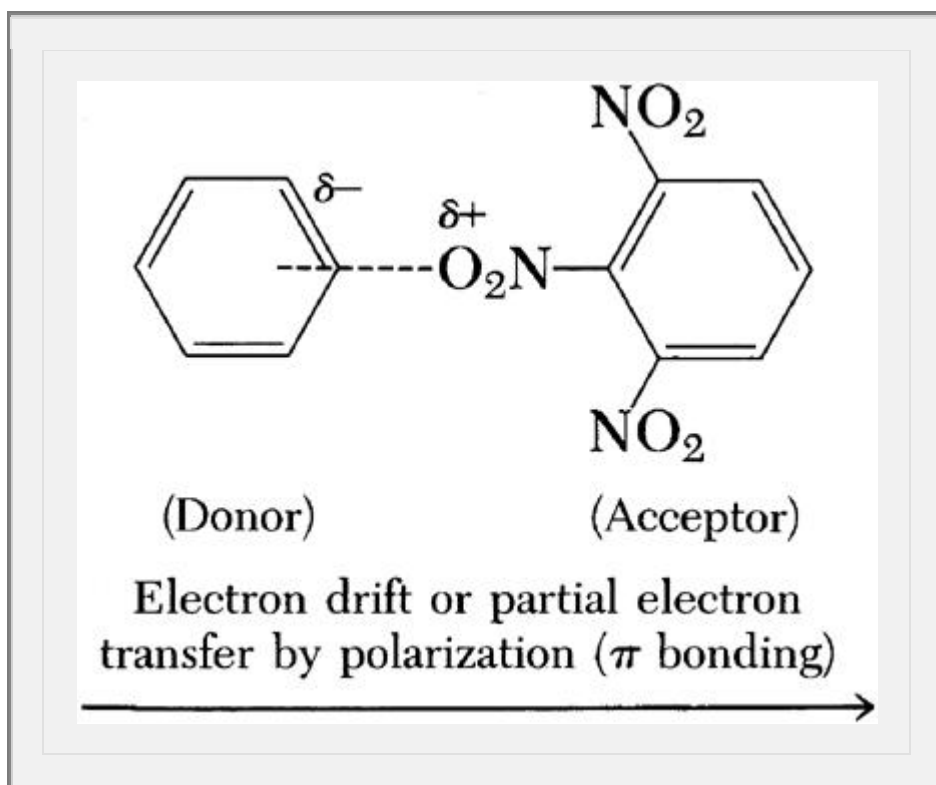
The type of bonding existing in molecular complexes in which hydrogen bonding plays no part is not fully understood,

P.201

but it may be considered for the present as involving an electron donor–acceptor mechanism corresponding to that in metal complexes but ordinarily much weaker.



Many organic complexes are so weak that they cannot be separated from their solutions as definite compounds, and they are often difficult to detect by chemical and physical means. The energy of attraction between the constituents is probably less than 5 kcal/mole for most organic complexes. Because the bond distance between the components of the complex is usually greater than 3 Å, a covalent link is not involved. Instead, one molecule polarizes the other, resulting in a type of ionic interaction or charge transfer, and these molecular complexes are often referred to as *charge transfer complexes*. For example, the polar nitro groups of trinitrobenzene induce a dipole in the readily polarizable benzene molecule, and the electrostatic interaction that results leads to complex formation:



X-ray diffraction studies of complexes formed between trinitrobenzene and aniline derivatives have shown that one of the nitro groups of trinitrobenzene lies over the benzene ring of the aniline molecule, the intermolecular distance between the two molecules being about 3.3 Å. This result strongly suggests that the interaction involves  $\pi$  bonding between the  $\pi$  electrons of the benzene ring and the electron-accepting nitro group.

A factor of some importance in the formation of molecular complexes is the steric requirement. If the approach and close association of the donor and acceptor molecules are hindered by steric factors, the complex is not likely to form. Hydrogen bonding and other effects must also be considered, and these are discussed in connection with the specific complexes considered on the following pages.

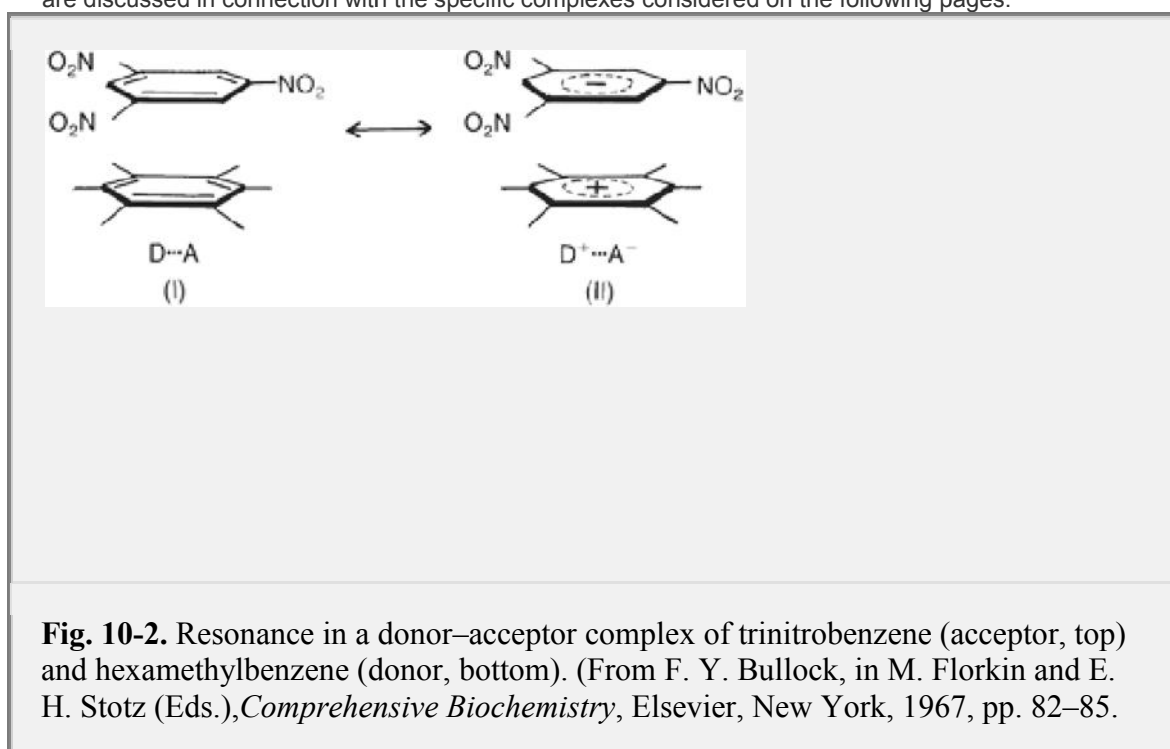


**Fig. 10-2.** Resonance in a donor–acceptor complex of trinitrobenzene (acceptor, top) and hexamethylbenzene (donor, bottom). (From F. Y. Bullock, in M. Florkin and E. H. Stotz (Eds.), *Comprehensive Biochemistry*, Elsevier, New York, 1967, pp. 82–85.

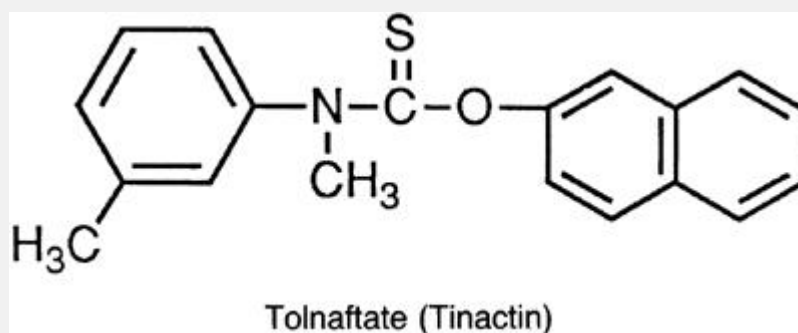
With permission.)

The difference between a *donor-acceptor* and a *charge transfer* complex is that in the latter type, resonance makes the main contribution to complexation, whereas in the former, London dispersion forces and dipole-dipole interactions contribute more to the stability of the complex. A resonance interaction is shown in Figure 10-2 as depicted by Bullock.<sup>8</sup> Trinitrobenzene is the acceptor, A, molecule and hexamethylbenzene is the donor, D. On the left side of the figure, weak dispersion and dipolar forces contribute to the interaction of A and D; on the right side of the figure, the interaction of A and D results from a significant transfer of charge, making the electron acceptor trinitrobenzene negatively charged ( $A^-$ ) and leaving the donor, hexamethylbenzene, positively charged ( $D^+$ ). The overall donor-acceptor complex is shown by the double-headed arrow to resonate between the uncharged  $D \dots A$  and the charged  $D^+ \dots A^-$  moieties. If, as in the case of hexamethylbenzene-trinitrobenzene, the resonance is fairly weak, having an intermolecular binding energy  $\Delta G$  of about  $-4700$  calories, the complex is referred to as a *donor-acceptor complex*. If, on the other hand, resonance between the charge transfer structure ( $D^+ \dots A^-$ ) and the uncharged species ( $D \dots A$ ) contributes greatly to the binding of the donor and acceptor molecule, the complex is called a *charge transfer complex*. Finally, those complexes bound together by van der Waals forces, dipole-dipole interactions, and hydrogen bonding but lacking charge transfer are known simply as *molecular complexes*. In both charge transfer and donor-acceptor complexes, new absorption bands occur in the spectra, as shown later in Figure 10-13. In this book we do not attempt to separate the first two classes, but rather refer to all interactions that produce absorption bands as charge transfer or as electron donor-acceptor complexes without distinction. Those complexes that do not show new bands are called molecular complexes.

Charge transfer complexes are of importance in pharmacy. Iodine forms 1:1 charge transfer complexes with the drugs disulfiram, chlomethiazole, and tolinaftate. These drugs have recognized pharmacologic actions of their own:

P.202

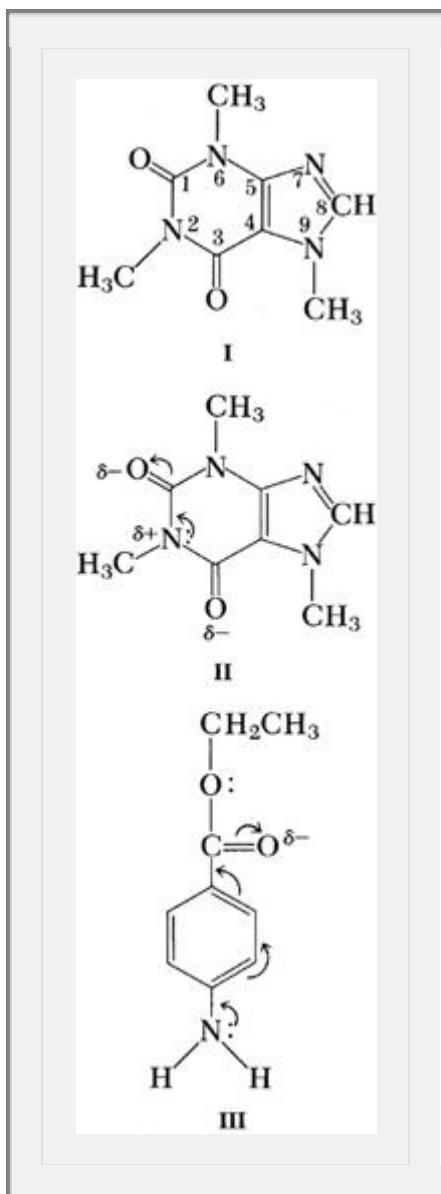
Disulfiram is used against alcohol addiction, chlomethiazole is a sedative-hypnotic and anticonvulsant, and tolinaftate is an antifungal agent. Each of these drugs possesses a nitrogen-carbon-sulfur moiety (see the accompanying structure of tolinaftate), and a complex may result from the transfer of charge from the pair of free electrons on the nitrogen and/or sulfur atoms of these drugs to the antibonding orbital of the iodine atom. Thus, by tying up iodine, molecules containing the  $N-C=S$  moiety inhibit thyroid action in the body.<sup>9</sup>



## Drug Complexes

Higuchi and his associates<sup>10</sup> investigated the complexing of caffeine with a number of acidic drugs. They attributed the interaction between caffeine and a drug such as a sulfonamide or a barbiturate to a dipole–dipole force or hydrogen bonding between the polarized carbonyl groups of caffeine and the hydrogen atom of the acid. A secondary interaction probably occurs between the nonpolar parts of the molecules, and the resultant complex is “squeezed out” of the aqueous phase owing to the great internal pressure of water. These two effects lead to a high degree of interaction.

The complexation of esters is of particular concern to the pharmacist because many important drugs belong to this class. The complexes formed between esters and amines, phenols, ethers, and ketones have been attributed to the hydrogen bonding between a nucleophilic carbonyl oxygen and an active hydrogen. This, however, does not explain the complexation of esters such as benzocaine, procaine, and tetracaine with caffeine, as reported by Higuchi et al.<sup>11</sup> There are no activated hydrogens on caffeine; the hydrogen in the number 8 position (formula I) is very weak ( $K_a = 1 \times 10^{-14}$ ) and is not likely to enter into complexation. It might be suggested that, in the caffeine molecule, a relatively positive center exists that serves as a likely site of complexation. The caffeine molecule is numbered in formula I for convenience in the discussion. As observed in formula II, the nitrogen at the 2 position presumably can become strongly electrophilic or acidic just as it is in an imide, owing to the withdrawal of electrons by the oxygens at positions 1 and 3. An ester such as benzocaine also becomes polarized (formula III) in such a way that the carboxyl oxygen is nucleophilic or basic. The complexation can thus occur as a result of a dipole–dipole interaction between the nucleophilic carboxyl oxygen of benzocaine and the electrophilic nitrogen of caffeine.



Caffeine forms complexes with organic acid *anions* that are more soluble than the pure xanthine, but the complexes formed with organic acids, such as gentisic acid, are less soluble than caffeine alone. Such insoluble complexes provide caffeine in a form that masks its normally bitter taste and should serve as a suitable state for chewable tablets. Higuchi and Pitman<sup>12</sup> synthesized 1:1 and 1:2 caffeine–gentisic acid complexes and measured their equilibrium solubility and rates of dissolution. Both the 1:1 and 1:2 complexes were less soluble in water than caffeine, and their dissolution rates were also less than that of caffeine. Chewable tablets formulated from these complexes should provide an extended-release form of the drug with improved taste.

York and Saleh<sup>13</sup> studied the effect of sodium salicylate on the release of benzocaine from topical vehicles, it being recognized that salicylates form molecular complexes with benzocaine. Complexation between drug and complexing agents can improve or impair drug absorption and bioavailability; the authors found that the presence of sodium salicylate significantly influenced the release of benzocaine, depending on the type of vehicle involved. The largest increase in absorption was observed for a water-miscible polyethylene glycol base.

P.203

**Table 10-3 Some Molecular Organic Complexes of Pharmaceutical Interest\***

Agent	Compounds That Form Complexes with the Agent Listed in the First Column
Polyethylene glycols	<i>m</i> -Hydroxybenzoic acid, <i>p</i> -hydroxybenzoic acid, salicylic acid, <i>o</i> -phthalic acid, acetylsalicylic acid, resorcinol, catechol, phenol, phenobarbital, iodine (in I <sub>2</sub> · KI solutions), bromine (in presence of HBr)
Povidone (polyvinylpyrrolidone, PVP)	Benzoic acid, <i>m</i> -hydroxybenzoic acid, <i>p</i> -hydroxybenzoic acid, salicylic acid, sodium salicylate, <i>p</i> -aminobenzoic acid, mandelic acid, sulfathiazole, chloramphenicol, phenobarbital
Sodium carboxymethylcellulose	Quinine, benadryl, procaine, pyribenzamine
Oxytetracycline and tetracycline	<i>N</i> -Methylpyrrolidone, <i>N,N</i> -dimethylacetamide, $\gamma$ -valerolactone, $\gamma$ -butyrolactone, sodium <i>p</i> -aminobenzoate, sodium salicylate, sodium <i>p</i> -hydroxybenzoate, sodium saccharin, caffeine
<p>*Compiled from the results of T. Higuchi et al., J. Am. Pharm. Assoc. Sci. Ed. <b>43</b>, 393, 398, 456, 1954; <b>44</b>, 668, 1955; <b>45</b>, 157, 1956; <b>46</b>, 458, 587, 1957; and J. L. Lach et al., Drug Stand. <b>24</b>, 11, 1956. An extensive table of acceptor and donor molecules that form aromatic molecular complexes was compiled by L. J. Andrews, Chem. Rev. <b>54</b>, 713, 1954. Also refer to T. Higuchi and K. A. Connors, Phase Solubility Techniques. <i>Advances in Analytical Chemistry and Instrumentation</i>, in C. N. Reilley (Ed.), Wiley, New York, 1965, pp. 117–212.</p>	

### Polymer Complexes

Polyethylene glycols, polystyrene, carboxymethylcellulose, and similar polymers containing nucleophilic oxygens can form complexes with various drugs. The incompatibilities of certain polyethers, such as the Carbowaxes, Pluronic, and Tweens with tannic acid, salicylic acid, and phenol, can be attributed to these interactions. Marcus<sup>14</sup> reviewed some of the interactions that may occur in suspensions, emulsions, ointments, and suppositories. The incompatibility may be manifested as a precipitate, flocculate, delayed biologic absorption, loss of preservative action, or other undesirable physical, chemical, and pharmacologic effects.

Plaizier-Vercammen and De Nève<sup>15</sup> studied the interaction of povidone (PVP) with ionic and neutral aromatic compounds. Several factors affect the binding to PVP of substituted benzoic acid and nicotine derivatives. Although ionic strength has no influence, the binding increases in phosphate buffer solutions and decreases as the temperature is raised.

Crosspovidone, a cross-linked insoluble PVP, is able to bind drugs owing to its dipolar character and porous structure. Frömring et al.<sup>16</sup> studied the interaction of crosspovidone with acetaminophen, benzocaine, benzoic acid, caffeine, tannic acid, and papaverine hydrochloride, among other drugs. The interaction is mainly due to any phenolic groups on the drug. Hexylresorcinol shows exceptionally strong binding, but the interaction is less than 5% for most drugs studied (32 drugs). Crosspovidone is a disintegrant in pharmaceutical granules and tablets. It does not interfere with gastrointestinal absorption because the binding to drugs is reversible.

Solutes in parenteral formulations may migrate from the solution and interact with the wall of a polymeric container. Hayward et al.<sup>17</sup> showed that the ability of a polyolefin container to interact with drugs depends linearly on the octanol–water partition coefficient of the drug. For parabens and drugs that exhibit fairly significant hydrogen bond donor properties, a correction term related to hydrogen-bond formation is needed. Polymer–drug container interactions may result in loss of the active component in liquid dosage forms.

Polymer–drug complexes are used to modify biopharmaceutical parameters of drugs; the dissolution rate of ajmaline is enhanced by complexation with PVP. The interaction is due to the aromatic ring of ajmaline and the amide groups of PVP to yield a dipole–dipole-induced complex.<sup>18</sup>

Some molecular organic complexes of interest to the pharmacist are given in Table 10-3. (Complexes involving caffeine are listed in Table 10-6.)

## **Inclusion Compounds**

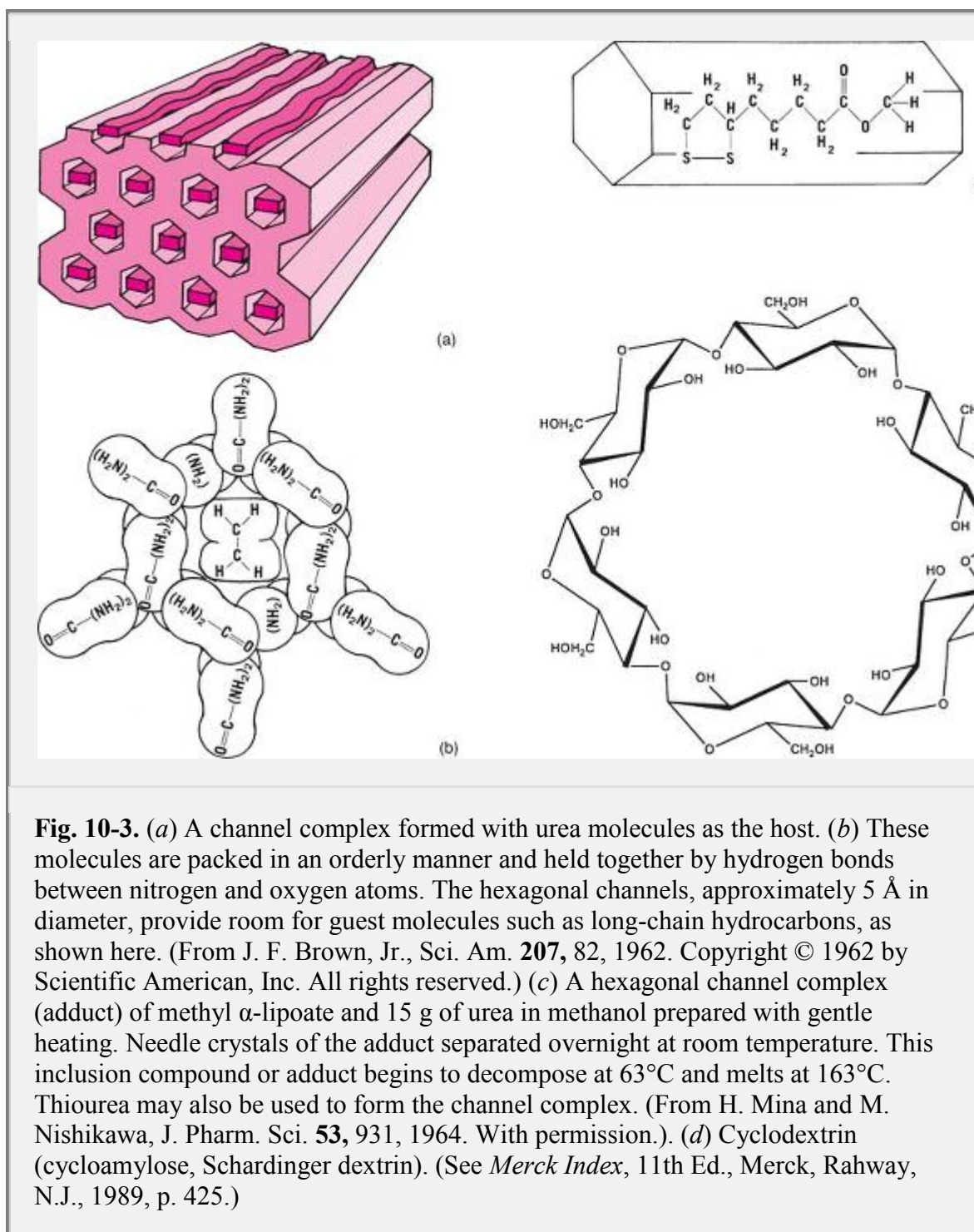
The class of addition compounds known as *inclusion* or *occlusion* compounds results more from the architecture of molecules than from their chemical affinity. One of the constituents of the complex is trapped in the open lattice or cage-like crystal structure of the other to yield a stable arrangement.

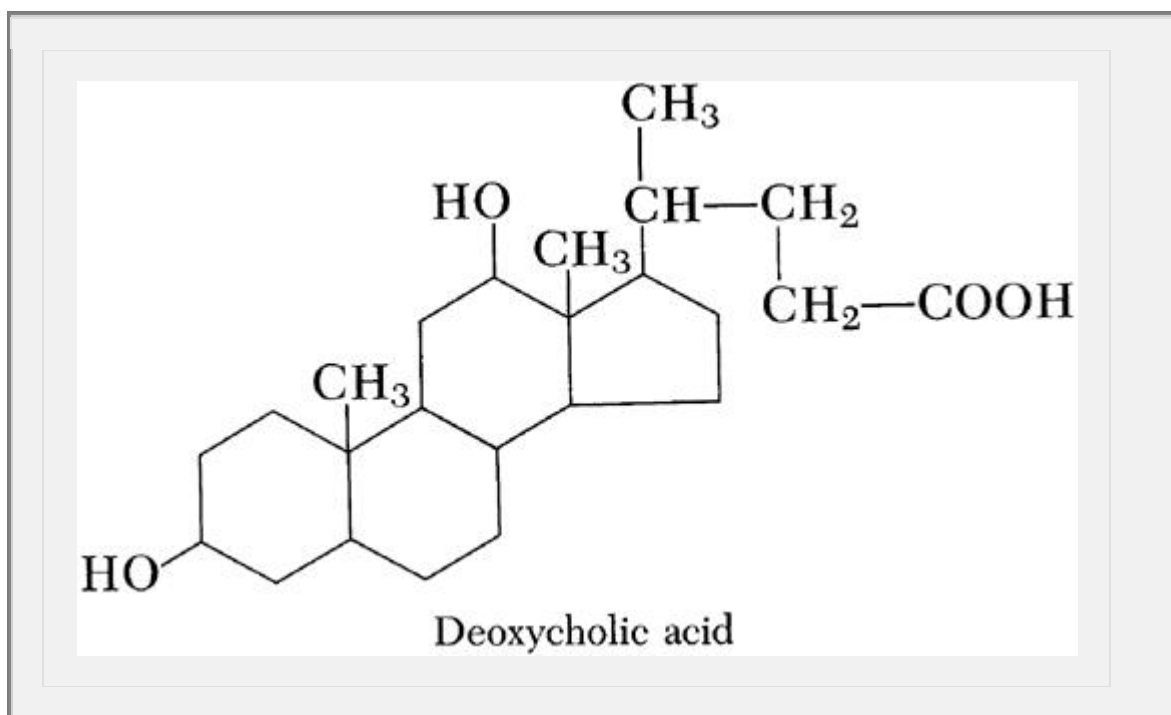
### **Channel Lattice Type**

The *cholic acids* (bile acids) can form a group of complexes principally involving deoxycholic acid in combination with paraffins, organic acids, esters, ketones, and aromatic compounds and with solvents such as ether, alcohol, and dioxane. The crystals of deoxycholic acid are arranged to form a channel into which the complexing molecule can fit (Fig. 10-3). Such stereospecificity should permit the resolution of optical isomers. In fact, camphor has been partially resolved by complexation with deoxycholic acid, and *ddl*-terpineol has been resolved by the use of digitonin, which

P.204

occludes certain molecules in a manner similar to that of deoxycholic acid:





Urea and thiourea also crystallize in a channel-like structure permitting enclosure of unbranched paraffins, alcohols, ketones, organic acids, and other compounds, as shown in Figure 10-3a and *b*. The well-known starch-iodine solution is a channel-type complex consisting of iodine molecules entrapped within spirals of the glucose residues.

Forman and Grady<sup>19</sup> found that monostearin, an interfering substance in the assay of dienestrol, could be extracted easily from dermatologic creams by channel-type inclusion in urea. They felt that urea inclusion might become a general approach for separation of long-chain compounds in assay methods. The authors reviewed the earlier literature on urea inclusion of straight-chain hydrocarbons and fatty acids.

P.205

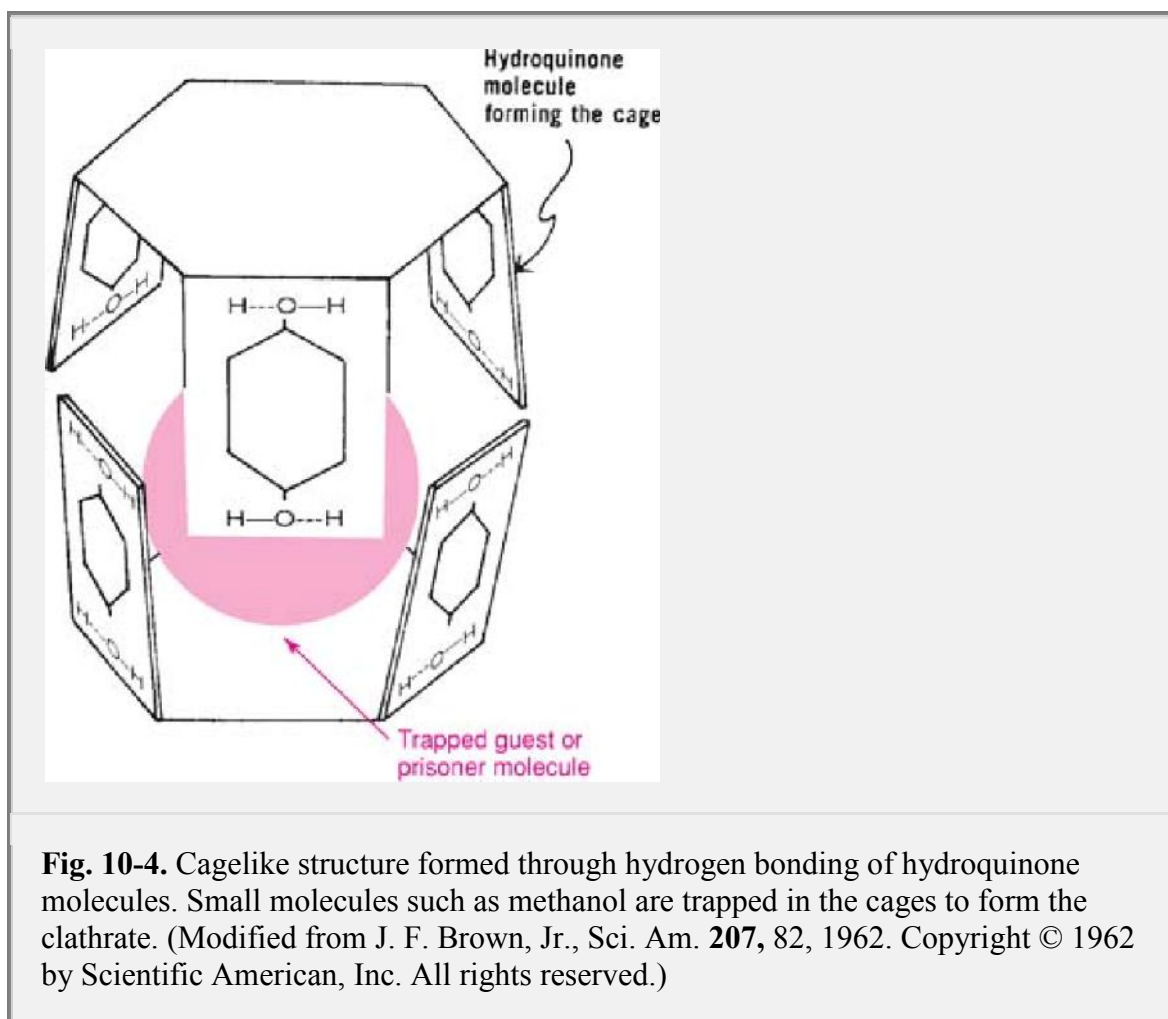
### **Layer Type**

Some compounds, such as the clay montmorillonite, the principal constituent of bentonite, can trap hydrocarbons, alcohols, and glycols between the layers of their lattices.<sup>20</sup> Graphite can also intercalate compounds between its layers.

### **Clathrates<sup>21</sup>**

The clathrates crystallize in the form of a cage-like lattice in which the coordinating compound is entrapped. Chemical bonds are not involved in these complexes, and only the molecular size of the encaged component is of importance. Ketelaar<sup>22</sup> observed the analogy between the stability of a clathrate and the confinement of a prisoner. The stability of a clathrate is due to the strength of the structure, that is, to the high energy that must be expended to decompose the compound, just as a prisoner is confined by the bars that prevent escape.

Powell and Palin<sup>23</sup> made a detailed study of clathrate compounds and showed that the highly toxic agent hydroquinone (quinol) crystallizes in a cage-like hydrogen-bonded structure, as seen in Figure 10-4. The holes have a diameter of 4.2 Å and permit the entrapment of one small molecule to about every two quinol molecules. Small molecules such as methyl alcohol, CO<sub>2</sub>, and HCl may be trapped in these cages, but smaller molecules such as H<sub>2</sub> and larger molecules such as ethanol cannot be accommodated. It is possible that clathrates may be used to resolve optical isomers and to bring about other processes of molecular separation.



One official drug, warfarin sodium, United States Pharmacopeia, is a clathrate of water, isopropyl alcohol, and sodium warfarin in the form of a white crystalline powder.

### **Monomolecular Inclusion Compounds: Cyclodextrins**

Inclusion compounds were reviewed by Frank.<sup>24a</sup> In addition to channel- and cage-type (clathrate) compounds, Frank added classes of *mono-* and *macromolecular* inclusion compounds. Monomolecular inclusion compounds involve the entrapment of a single guest molecule in the cavity of one host molecule. Monomolecular host structures are represented by the cyclodextrins (CD). These compounds are cyclic oligosaccharides containing a minimum of six D-(+)-glucopyranose units attached by  $\alpha$ -1,4 linkages produced by the action on starch of *Bacillus macerans* amylase. The natural  $\alpha$ -,  $\beta$ -, and  $\gamma$ -cyclodextrins ( $\alpha$ -CD,  $\beta$ -CD, and  $\gamma$ -CD, respectively) consist of six, seven, and eight units of glucose, respectively.

Their ability to form inclusion compounds in aqueous solution is due to the typical arrangement of the glucose units (see Fig. 10-3d). As observed in cross section in the figure, the cyclodextrin structure forms a torus or doughnut ring. The molecule actually exists as a truncated cone, which is seen in Figure 10-5a; it can accommodate molecules such as mitomycin C to form inclusion compounds (Fig. 10-5b). The interior of the cavity is relatively hydrophobic because of the  $\text{CH}_2$  groups, whereas the cavity entrances are hydrophilic owing to the presence of the primary and secondary hydroxyl groups.<sup>25,26</sup>  $\alpha$ -CD has the smallest cavity (internal diameter almost 5 Å).  $\beta$ -CD and  $\gamma$ -CD are the most useful for pharmaceutical technology owing to their larger cavity size (internal diameter almost 6 Å and 8 Å, respectively). Water inside the cavity tends to be squeezed out and to be replaced by more hydrophobic species. Thus, molecules of appropriate size and stereochemistry can be included in the cyclodextrin cavity by

hydrophobic interactions. Complexation does not ordinarily involve the formation of covalent bonds. Some drugs may be too large to be accommodated totally in the cavity. As shown in Figure 10-5b, mitomycin C interacts with  $\gamma$ -CD at one side of the torus. Thus, the aziridine ring

### Key Concept

#### Cyclodextrins

According to Davis and Brewster,<sup>24b</sup> "Cyclodextrins are cyclic oligomers of glucose that can form water-soluble inclusion complexes with small molecules and portions of large compounds. These biocompatible, cyclic oligosaccharides do not elicit immune responses and have low toxicities in animals and humans. Cyclodextrins are used in pharmaceutical applications for numerous purposes, including improving the bioavailability of drugs. Of specific interest is the use of cyclodextrin-containing polymers to provide unique capabilities for the delivery of nucleic acids." Davis and Brewster<sup>24b</sup> discuss cyclodextrin-based therapeutics and possible future applications, and review the use of cyclodextrin-containing polymers in drug delivery.

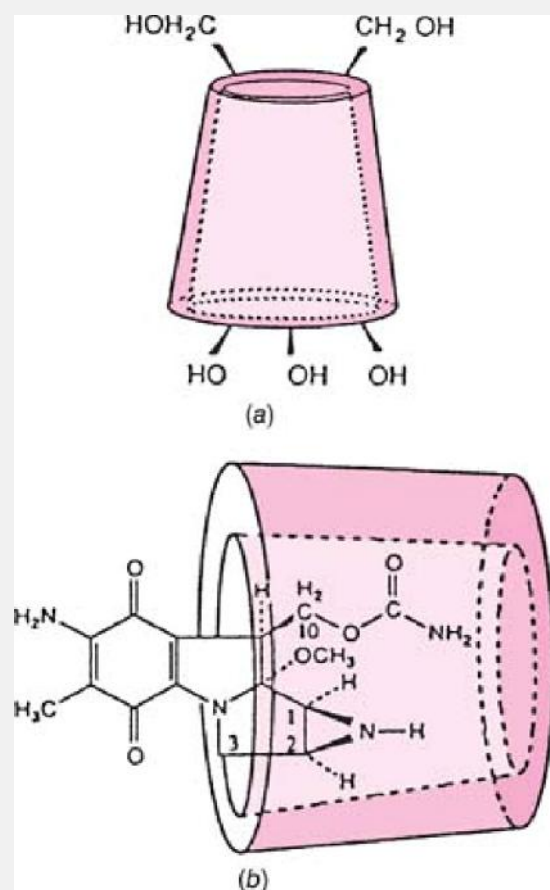
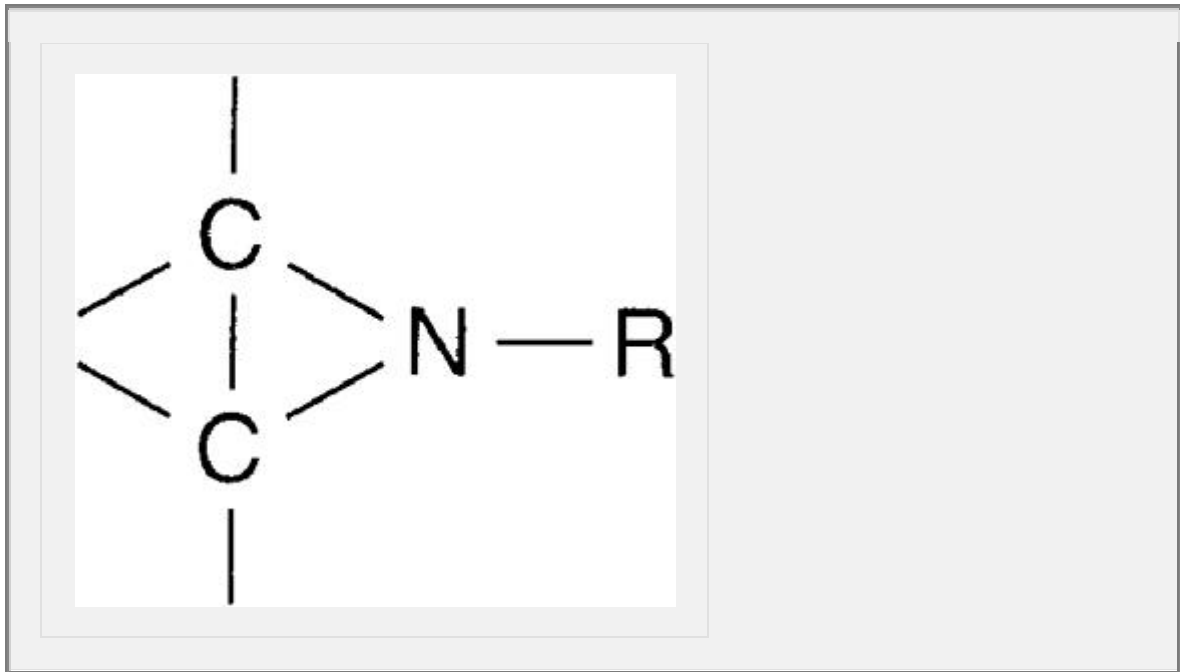


**Fig. 10-5.** (a) Representation of cyclodextrin as a truncated cone. (b) Mitomycin C partly enclosed in cyclodextrin to form an inclusion complex. (From O. Beckers, *Int. J. Pharm.* **52**, 240, 247, 1989. With permission.)



of mitomycin C is protected from degradation in acidic solution.<sup>27</sup>Bakensfield et al.<sup>28</sup> studied the inclusion of indomethacin with  $\beta$ -CD using a  $^1\text{H-NMR}$  technique. The *p*-chlorobenzoyl part of indomethacin (shaded part of Fig. 10-6) enters the  $\beta$ -CD ring, whereas the substituted indole moiety (the remainder of the molecule) is too large for inclusion and rests against the entrance of the CD cavity.

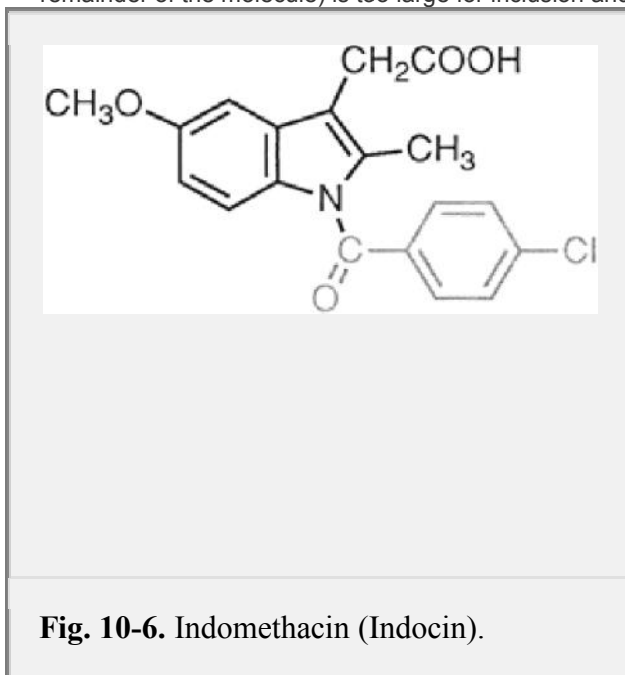


**Fig. 10-6.** Indomethacin (Indocin).

Cyclodextrins are studied as solubilizing and stabilizing agents in pharmaceutical dosage forms. Lach and associates<sup>29</sup> used cyclodextrins to trap, stabilize, and solubilize sulfonamides, tetracyclines, morphine, aspirin, benzocaine, ephedrine, reserpine, and testosterone. The aqueous solubility of retinoic acid (0.5 mg/liter), a drug used topically in the treatment of acne,<sup>30</sup> is increased to 160 mg/liter by complexation with  $\beta$ -CD. Dissolution rate plays an important role in bioavailability of drugs, fast dissolution usually favoring absorption. Thus, the dissolution rates of famotidine,<sup>31</sup> a potent drug in the treatment of gastric and duodenal ulcers, and that of tolbutamide, an oral antidiabetic drug, are both increased by complexation with  $\beta$ -cyclodextrin.<sup>32</sup>

Cyclodextrins may increase or decrease the reactivity of the guest molecule depending on the nature of the reaction and the orientation of the molecule within the CD cavity. Thus,  $\alpha$ -cyclodextrin tends to favor

pH-dependent hydrolysis of indomethacin in aqueous solution, whereas  $\beta$ -cyclodextrin inhibits it.<sup>28</sup> Unfortunately, the water solubility of  $\beta$ -CD (1.8 g/100 mL at 25°C) is often insufficient to stabilize drugs at therapeutic doses and is also associated with nephrotoxicity when CD is administered by parenteral routes.<sup>33</sup> The relatively low aqueous solubility of the cyclodextrins may be due to the formation of intramolecular hydrogen bonds between the hydroxyl groups (see Fig. 10-3d), which prevent their interaction with water molecules.<sup>34</sup>

Derivatives of the natural crystalline CD have been developed to improve aqueous solubility and to avoid toxicity. Partial methylation (alkylation) of some of the OH groups in CD reduces the intermolecular hydrogen bonding, leaving some OH groups free to interact with water, thus increasing the aqueous solubility of CD.<sup>34</sup> According to Müller and Brauns,<sup>35</sup> a low degree of alkyl substitution is preferable. Derivatives with a high degree of substitution lower the surface tension of water, and this has been correlated with the hemolytic activity observed in some CD derivatives. Amorphous derivatives of  $\beta$ -CD and  $\gamma$ -CD are more effective as solubilizing agents for sex hormones than the parent cyclodextrins. Complexes of testosterone with amorphous hydroxypropyl  $\beta$ -CD allow an efficient transport of hormone into the circulation when given sublingually.<sup>36</sup> This route avoids both metabolism of the drug in the intestines and rapid *first-pass* decomposition in the liver (see Chapter 15), thus improving bioavailability.

In addition to hydrophilic derivatives, hydrophobic forms of  $\beta$ -CD have been found useful as sustained-release drug carriers. Thus, the release rate of the water-soluble calcium antagonist diltiazem was significantly decreased by complexation with ethylated  $\beta$ -CD. The release rate was controlled by mixing hydrophobic and hydrophilic derivatives of cyclodextrins at several ratios.<sup>37</sup> Ethylated  $\beta$ -CD has also been used to retard the delivery of isosorbide dinitrate, a vasodilator.<sup>38</sup>

Cyclodextrins may improve the organoleptic characteristics of oral liquid formulations. The bitter taste of suspensions of femoxetine, an antidepressant, is greatly suppressed by complexation of the drug with  $\beta$ -cyclodextrin.<sup>39</sup>

P.207

## Molecular Sieves

Macromolecular inclusion compounds, or *molecular sieves* as they are commonly called, include zeolites, dextrans, silica gels, and related substances. The atoms are arranged in three dimensions to produce cages and channels. Synthetic zeolites may be made to a definite pore size so as to separate molecules of different dimensions, and they are also capable of ion exchange. See the review article by Frank<sup>24a</sup> for a detailed discussion of inclusion compounds.

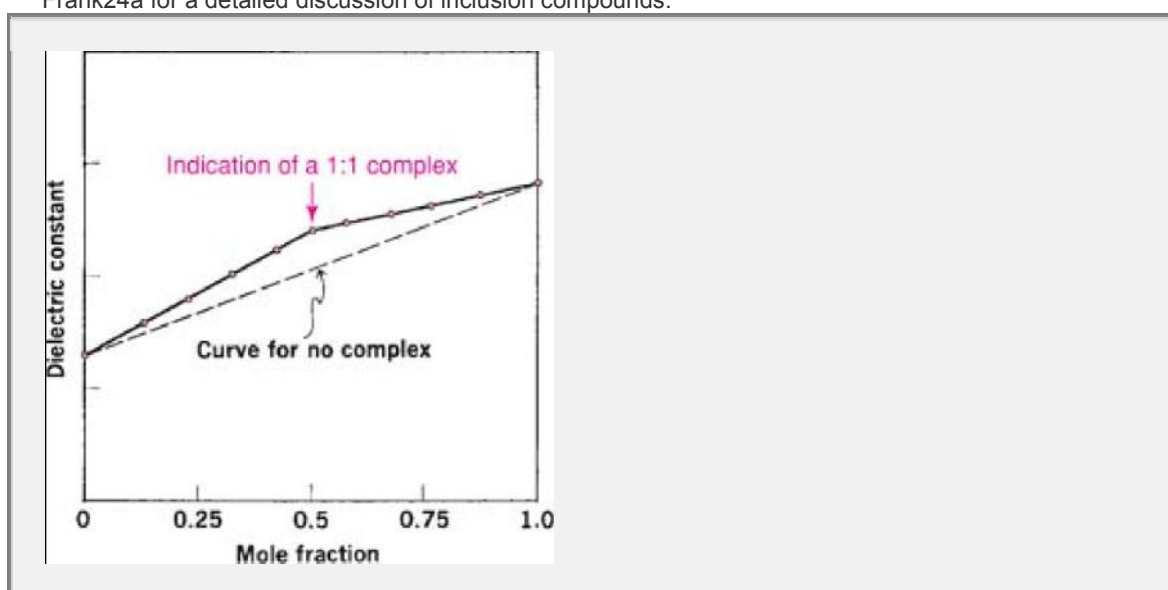


**Fig. 10-7.** A plot of an additive property against mole fraction of one of the species in which complexation between the species has occurred. The dashed line is that expected if no complex had formed. (Refer to C. H. Giles et al., J. Chem. Soc., 1952, 3799, for similar figures.)

## Methods of Analysis<sup>40</sup>

A determination of the *stoichiometric ratio* of ligand to metal or donor to acceptor and a quantitative expression of the *stability constant* for complex formation are important in the study and application of coordination compounds. A limited number of the more important methods for obtaining these quantities is presented here.

### **Method of Continuous Variation**

Job<sup>41</sup> suggested the use of an additive property such as the spectrophotometric extinction coefficient (dielectric constant or the square of the refractive index may also be used) for the measurement of complexation. If the property for two species is sufficiently different and if no interaction occurs when the components are mixed, then the value of the property is the weighted mean of the values of the separate species in the mixture. This means that if the additive property, say dielectric constant, is plotted against the mole fraction from 0 to 1 for one of the components of a mixture where no complexation occurs, a linear relationship is observed, as shown by the dashed line in Figure 10-7. If solutions of two species *A* and *B* of equal molar concentration (and hence of a fixed total concentration of the species) are mixed and if a complex forms between the two species, the value of the additive property will pass through a maximum (or minimum), as shown by the upper curve in Figure 10-7. For a constant total concentration of *A* and *B*, the complex is at its greatest concentration at a point where the species *A* and *B* are combined in the ratio in which they occur in the complex. The line therefore shows a break or a change in slope at the mole fraction corresponding to the complex. The change in slope occurs at a mole fraction of 0.5 in Figure 10-7, indicating a complex of the 1:1 type.

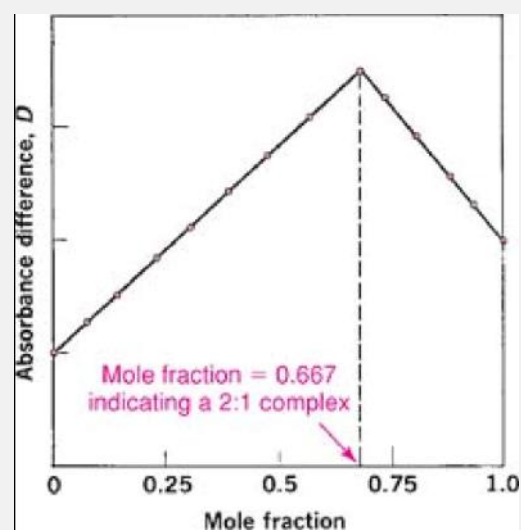


**Fig. 10-8.** A plot of absorbance difference against mole fraction showing the result of complexation.

When spectrophotometric absorbance is used as the physical property, the observed values obtained at various mole fractions when complexation occurs are usually subtracted from the corresponding values that would have been expected had no complex resulted. This difference, *D*, is then plotted against mole fraction, as shown in Figure 10-8. The molar ratio of the complex is readily obtained from such a curve.

By means of a calculation involving the concentration and the property being measured, the stability constant of the formation can be determined by a method described by Martell and Calvin.<sup>42</sup> Another method, suggested by Bent and French,<sup>43</sup> is given here.

If the magnitude of the measured property, such as absorbance, is proportional only to the concentration of the complex  $MA_n$ , the molar ratio of ligand  $A$  to metal  $M$  and the stability constant can be readily determined. The equation for complexation can be written as



and the stability constant as

$$K = \frac{[MA_n]}{[M][A]^n} \quad (10-4)$$

or, in logarithmic form,

$$\log [MA_n] = \log K + \log [M] + n \log [A] \quad (10-5)$$

where  $[MA_n]$  is the concentration of the complex,  $[M]$  is the

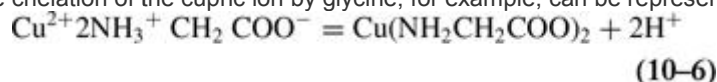
P.208

concentration of the uncomplexed metal,  $[A]$  is the concentration of the uncomplexed ligand,  $n$  is the number of moles of ligand combined with 1 mole of metal ion, and  $K$  is the equilibrium *stability* constant for the complex. The concentration of a metal ion is held constant while the concentration of ligand is varied, and the corresponding concentration,  $[MA_n]$ , of complex formed is obtained from the spectrophotometric analysis.<sup>41</sup> Now, according to equation (10-5), if  $\log [MA_n]$  is plotted against  $\log [A]$ , the slope of the line yields the stoichiometric ratio or the number  $n$  of ligand molecules coordinated to the metal ion, and the intercept on the vertical axis allows one to obtain the stability constant,  $K$ , because  $[M]$  is a known quantity.

Job restricted his method to the formation of a single complex; however, Vosburgh et al.<sup>44</sup> modified it so as to treat the formation of higher complexes in solution. Osman and Abu-Eittah<sup>45</sup> used spectrophotometric techniques to investigate 1:2 metal–ligand complexes of copper and barbiturates. A greenish-yellow complex is formed by mixing a blue solution of copper (II) with thiobarbiturates (colorless). By using the Job method, an apparent stability constant as well as the composition of the 1:2 complex was obtained.

### **pH Titration Method**

This is one of the most reliable methods and can be used whenever the complexation is attended by a change in pH. The chelation of the cupric ion by glycine, for example, can be represented as



Because two protons are formed in the reaction of equation (10-6), the addition of glycine to a solution containing cupric ions should result in a decrease in pH.

Titration curves can be obtained by adding a strong base to a solution of glycine and to another solution containing glycine and a copper salt and plotting the pH against the equivalents of base added. The results of such a potentiometric titration are shown in Figure 10-9. The curve for the metal–glycine mixture is well below that for the glycine alone, and the decrease in pH shows that complexation is occurring throughout most of the neutralization range. Similar results are obtained with other zwitterions and weak acids (or bases), such as *N,N'*-diacetylenediamine diacetic acid, which has been studied for its complexing action with copper and calcium ions.

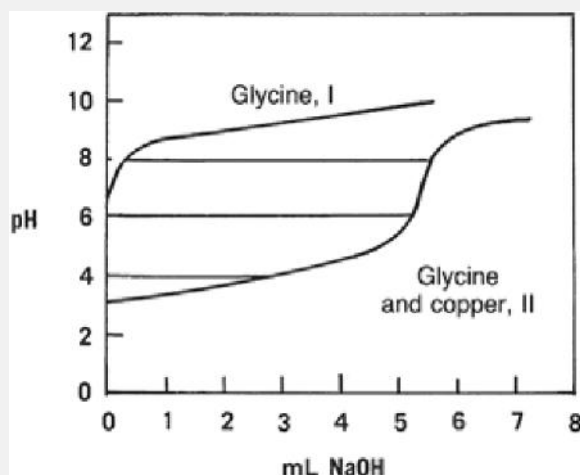
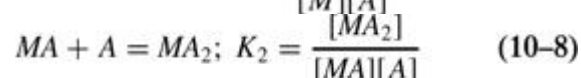
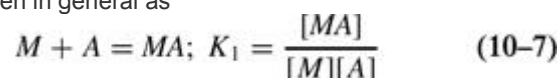
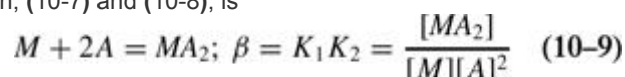


**Fig. 10-9.** Titration of glycine and of glycine in the presence of cupric ions. The difference in pH for a given quantity of base added indicates the occurrence of a complex.

The results can be treated quantitatively in the following manner to obtain stability constants for the complex. The two successive or stepwise equilibria between the copper ion or metal,  $M$ , and glycine or the ligand,  $A$ , can be written in general as



and the overall reaction, (10-7) and (10-8), is



Bjerrum<sup>46</sup> called  $K_1$  and  $K_2$  the *formation constants*, and the equilibrium constant,  $\beta$ , for the overall reaction is known as the *stability constant*. A quantity  $n$  may now be defined. It is the number of ligand molecules bound to a metal ion. The *average* number of ligand groups bound per metal ion present is therefore designated  $\bar{n}$  ( $n$  bar) and is written as

$$\bar{n} = \frac{\text{Total concentration of ligand bound}}{\text{Total concentration of metal ion}} \quad (10-10)$$

or

$$\bar{n} = \frac{[MA] + 2[MA_2]}{[M] + [MA] + [MA_2]} \quad (10-11)$$

Although  $n$  has a definite value for each species of complex (1 or 2 in this case), it may have any value between 0 and the largest number of ligand molecules bound, 2 in this case. The numerator of equation (10-11) gives the total concentration of ligand species bound. The second term in the numerator is multiplied by 2 because two molecules of ligand are contained in each molecule of the species,  $MA_2$ . The denominator gives the total concentration of metal present in all forms, both bound and free. For the special case in which  $\bar{n} = 1$ , equation (10-11) becomes

$$[MA] + 2[MA_2] = [M] + [MA] + [MA_2] \quad (10-12)$$

Employing the results in equations (10-9) and (10-12), we obtain the following relation:

$$\beta = K_1 K_2 = \frac{1}{[A]^2} \text{ or } \log \beta = -2 \log[A]$$

and finally

$$p[A] = \frac{1}{2} \log \beta \text{ at } \bar{n} = 1 \quad (10-13)$$

P.209

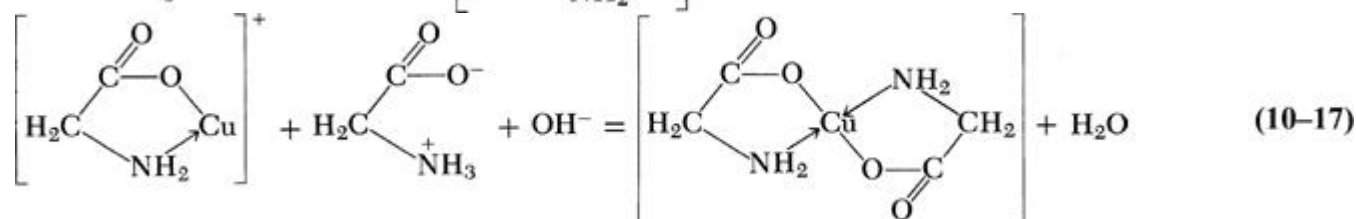
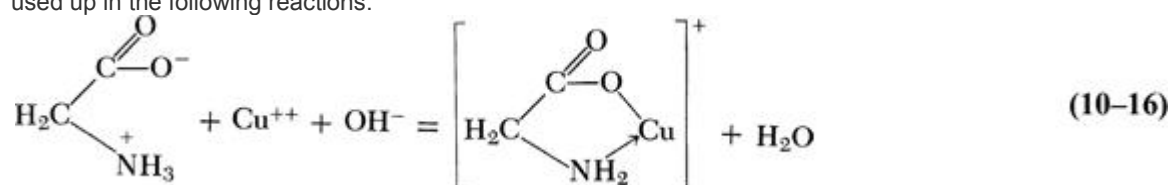
where  $p[A]$  is written for  $-\log [A]$ . Bjerrum also showed that, to a first approximation,

$$p[A] = \log K_1 \text{ at } \bar{n} = \frac{1}{2} \quad (10-14)$$

$$p[A] = \log K_2 \text{ at } \bar{n} = \frac{3}{2} \quad (10-15)$$

It should now be possible to obtain the individual complex formation constants,  $K_1$  and  $K_2$ , and the overall stability constant,  $\beta$ , if one knows two values:  $[\bar{n}]$  and  $p[A]$ .

Equation (10-10) shows that the concentration of bound ligand must be determined before  $\bar{n}$  can be evaluated. The horizontal distances represented by the lines in Figure 10-9 between the titration curve for glycine alone (curve I) and for glycine in the presence of  $\text{Cu}^{2+}$  (curve II) give the amount of alkali used up in the following reactions:



This quantity of alkali is exactly equal to the concentration of ligand bound at any pH, and, according to equation (10-10), when divided by the total concentration of metal ion, gives the value of  $[\bar{n}]$ .

The concentration of free glycine  $[A]$  as the "base"  $\text{NH}_2\text{CH}_2\text{COO}^-$  at any pH is obtained from the acid dissociation expression for glycine:



$$K_a = \frac{[\text{H}_3\text{O}^+][\text{NH}_2\text{CH}_2\text{COO}^-]}{[\text{NH}_3^+\text{CH}_2\text{COO}^-]} \quad (10-18)$$

or

$$[\text{NH}_2\text{CH}_2\text{COO}^-], = [A] = \frac{K_a[HA]}{[\text{H}_3\text{O}^+]} \quad (10-19)$$

The concentration  $[\text{NH}_3^+ \text{CH}_2\text{COO}^-]$ , or  $[HA]$ , of the acid species at any pH is taken as the difference between the initial concentration,  $[HA]_{\text{init}}$ , of glycine and the concentration,  $[\text{NaOH}]$ , of alkali added. Then

$$[A] = K_a \frac{[HA]_{\text{init}} - [\text{NaOH}]}{[\text{H}_3\text{O}^+]} \quad (10-20)$$

or

$$-\log, [A] = p[A] = pK_a - \text{pH} - \log, ([HA]_{\text{init}} - [\text{NaOH}]) \quad (10-21)$$

where  $[A]$  is the concentration of the ligand glycine.

### Example 10-1

#### Calculate Average Number of Ligands

If 75-mL samples containing  $3.34 \times 10^{-2}$  mole/liter of glycine hydrochloride alone and in combination with  $9.45 \times 10^{-3}$  mole/liter of cupric ion are titrated with 0.259 N NaOH, the two

curves I and II, respectively, in Figure 10-9 are obtained. Compute  $\bar{n}$  and  $p[A]$  at pH 3.50 and pH 8.00. The  $pK_a$  of glycine is 9.69 at 30°C.

- a. From Figure 10-9, the horizontal distance at pH 3.50 for the 75-mL sample is 1.60 mL NaOH or  $2.59 \times 10^{-4}$  mole/mL  $\times 1.60 = 4.15 \times 10^{-4}$  mole. For a 1-liter sample, the value is  $5.54 \times 10^{-3}$  mole. The total concentration of copper ion per liter is  $9.45 \times 10^{-3}$  mole, and from equation (10-10),  $[\bar{n}]$  is given by

$$\bar{n} = \frac{5.54 \times 10^{-3}}{9.45 \times 10^{-3}} = 0.59$$

From equation (10-21),

$$p[A] = 9.69 - 3.50 - \log[(3.34 \times 10^{-2}) - (5.54 \times 10^{-3})] = 7.75$$

- b. At pH 8.00, the horizontal distance between the two curves I and II in Figure 10-9 is equivalent to 5.50 mL of NaOH in the 75-mL sample, or  $2.59 \times 10^{-4} \times 5.50 \times 1000/75 = 19.0 \times 10^{-3}$  mole/liter. We have

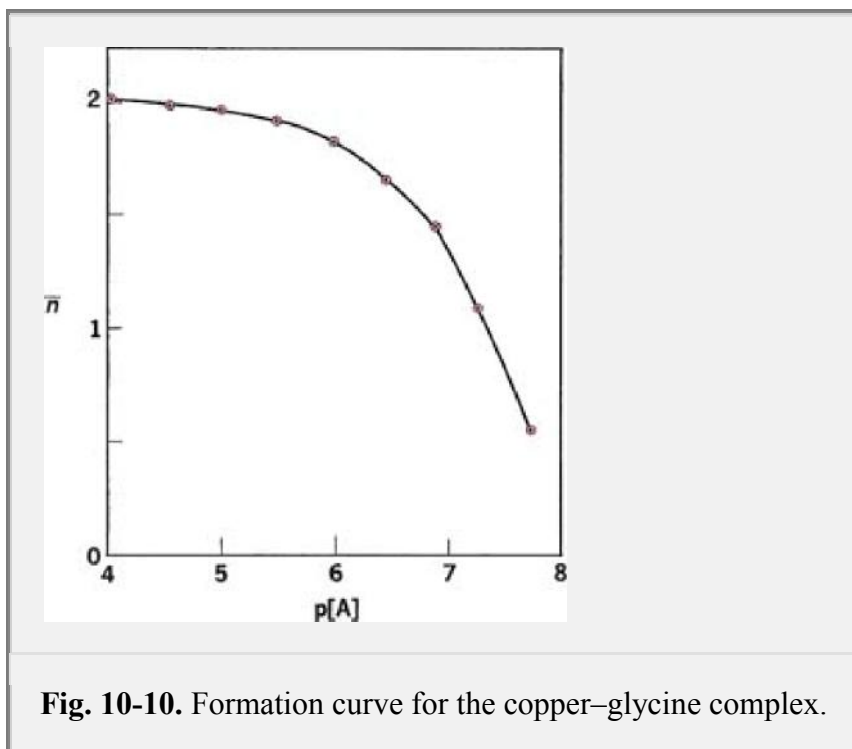
$$\bar{n} = \frac{19.0 \times 10^{-3}}{9.45 \times 10^{-3}} = 2.01$$

$$p[A] = 9.69 - 8.00 - \log[(3.34 \times 10^{-2}) - (1.90 \times 10^{-2})] = 3.53$$

The values of  $[\bar{n}]$  and  $p[A]$  at various pH values are then plotted as shown in Figure 10-10. The curve that is obtained is known as a *formation curve*. It is seen to reach a limit at  $[\bar{n}] = 2$ , indicating that the maximum number of glycine molecules that can combine with one atom of copper is 2. From this curve at  $[\bar{n}] = 0.5$ , at  $[\bar{n}] = 3/2$ , and at  $[\bar{n}] = 1.0$ , the approximate values for  $\log K_1$ ,  $\log K_2$ , and  $\log \beta$ , respectively, are obtained.

P.210

A typical set of data for the complexation of glycine by copper is shown in Table 10-4. Values of  $\log K_1$ ,  $\log K_2$ , and  $\log \beta$  for some metal complexes of pharmaceutical interest are given in Table 10-5.



Pecar et al.<sup>47</sup> described the tendency of pyrrolidone 5-hydroxamic acid to bind the ferric ion to form mono, bis, and tris chelates. These workers later studied the thermodynamics of these chelates using a potentiometric method to determine stability constants. The method employed by Pecar et al. is known as the *Schwarzenbach method* and can be used instead of the potentiometric method described here when complexes are unusually stable. Sandmann and Luk<sup>48</sup> measured the stability constants for lithium catecholamine complexes by potentiometric titration of the free lithium ion. The results demonstrated that lithium forms complexes with the zwitterionic species of catecholamines at pH 9 to 10 and with deprotonated forms at pH values above 10. The interaction with lithium depends on the dissociation of the phenolic oxygen of catecholamines. At physiologic pH, the protonated species show no significant complexation. Some lithium salts, such as lithium carbonate, lithium chloride, and lithium citrate, are used in psychiatry.

**Table 10-4 Potentiometric Titration of Glycine Hydrochloride ( $3.34 \times 10^{-2}$  Mole/Liter,  $pK_a$ , 9.69) and Cupric Chloride ( $9.45 \times 10^{-3}$  Mole/Liter) in 75-mL Samples Using 0.259 N NaOH at 30°C\***

pH	$\Delta$ (mL NaOH) (per 75-mL Sample)	Moles OH <sup>-</sup> , MAComplexed (mole/liter)	[n with bar above]	p[A]
3.50	1.60	$5.54 \times 10^{-3}$	0.59	7.66
4.00	2.90	$10.1 \times 10^{-3}$	1.07	7.32
4.50	3.80	$13.1 \times 10^{-3}$	1.39	6.85
5.00	4.50	$15.5 \times 10^{-3}$	1.64	6.44

5.50	5.00	$17.3 \times 10^{-3}$	1.83	5.98
6.00	5.20	$18.0 \times 10^{-3}$	1.91	5.50
6.50	5.35	$18.5 \times 10^{-3}$	1.96	5.02
7.00	5.45	$18.8 \times 10^{-3}$	1.99	4.53
7.50	5.50	$19.0 \times 10^{-3}$	2.03	4.03
8.00	5.50	$19.0 \times 10^{-3}$	2.01	3.15

\*From the data in the last two columns, the formation curve, **Figure 10-10**, is plotted, and the following results are obtained from the curve:  $\log K_1 = 7.9$ ,  $\log K_2 = 6.9$ , and  $\log \beta = 14.8$  (average  $\log \beta$  from the literature at 25°C is about 15.3).

**Table 10-5 Selected Constants for Complexes Between Metal Ions and Organic Ligand\***

Organic Ligand	Metal Ion	$\log K_1$	$\log K_2$	$\log, \beta = \log K_1 K_2$
Ascorbic acid	$\text{Ca}^{2+}$	0.19	—	—
Nicotinamide	$\text{Ag}^+$	—	—	3.2
Glycine (aminoacetic acid)	$\text{Cu}^{2+}$	8.3	7.0	15.3
Salicylaldehyde	$\text{Fe}^{2+}$	4.2	3.4	7.6
Salicylic acid	$\text{Cu}^{2+}$	10.6	6.3	16.9
<i>p</i> -hydroxybenzoic acid	$\text{Fe}^{3+}$	15.2	—	—
Methyl salicylate	$\text{Fe}^{3+}$	9.7	—	—

Diethylbarbituric acid (barbital)	Ca <sup>2+</sup>	0.66	—	—
8-Hydroxyquinoline	Cu <sup>2+</sup>	15	14	29
Pteroylglutamic acid (folic acid)	Cu <sup>2+</sup>	—	—	7.8
Oxytetracycline	Ni <sup>2+</sup>	5.8	4.8	10.6
Chlortetracycline	Fe <sup>3+</sup>	8.8	7.2	16.0

\*From J. Bjerrum, G. Schwarzenback, and L. G. Sillen, *Stability Constants, Part I, Organic Ligands*, The Chemical Society, London, 1957.

Agrawal et al.<sup>49</sup> applied a pH titration method to estimate the average number of ligand groups per metal ion, [ $\bar{n}$  with bar above], for several metal–sulfonamide chelates in dioxane–water. The maximum [ $\bar{n}$  with bar above] values obtained indicate 1:1 and 1:2 complexes.

P.211

The linear relationship between the  $pK_a$  of the drugs and the log of the stability constants of their corresponding metal ion complexes shows that the more basic ligands (drugs) give the more stable chelates with cerium (IV), palladium (II), and copper (II). A potentiometric method was described in detail by Connors et al.<sup>50</sup> for the inclusion-type complexes formed between  $\alpha$ -cyclodextrin and substituted benzoic acids.

### **Distribution Method**

The method of distributing a solute between two immiscible solvents can be used to determine the stability constant for certain complexes. The complexation of iodine by potassium iodide may be used as an example to illustrate the method. The equilibrium reaction in its simplest form is



Additional steps also occur in polyiodide formation; for example,  $2I^- + 2I_2$  [right harpoon over left harpoon]  $I_6^{2-}$  may occur at higher concentrations, but it need not be considered here.

#### **Example 10-2**

##### **Free and Total Iodine**

When iodine is distributed between water (w) at 25°C and carbon disulfide as the organic phase (o), as depicted in Figure 10-11, the distribution constant  $K(o/w) = C_o/C_w$  is found to be 625. When it is distributed between a 0.1250 M solution of potassium iodide and carbon disulfide, the concentration of iodine in the organic solvent is found to be 0.1896 mole/liter. When the aqueous KI solution is analyzed, the concentration of iodine is found to be 0.02832 mole/liter.

In summary, the results are as follows:

- Total concentration of  $I_2$  in the aqueous
- layer (free + complexed iodine): 0.02832, mole/liter

- Total concentration of KI in the aqueous
  - layer (free + complexed KI): 0.1250 mole/liter
- Concentration of I<sub>2</sub> in the CS<sub>2</sub> layer (free): 0.1896 mole/liter
  - Distribution coefficient,  $K(o/w) = [I_2]_o/[I_2]_w = 625$

The species common to both phases is the free or uncomplexed iodine; the distribution law expresses only the concentration of *free* iodine, whereas a chemical analysis yields the *total* concentration of iodine in the aqueous phase. The concentration of free iodine in the aqueous phase is obtained as follows:

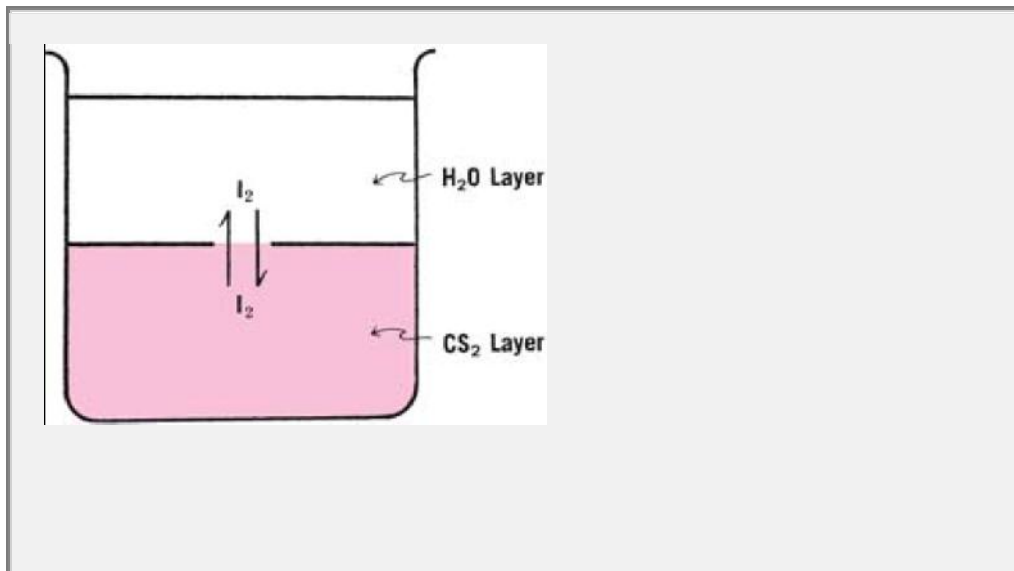


**Fig. 10-11.** The distribution of iodine between water and carbon disulfide.

$$[I_2]_w = \frac{[I_2]_o}{K(o/w)} = \frac{0.1896}{625} = 3.034 \times 10^{-4} \text{ mole/liter}$$

To obtain the concentration of iodine in the complex and hence the concentration of the complex, [I<sub>3</sub>], one subtracts the free iodine from the total iodine of the aqueous phase:

$$\begin{aligned} [I_2]_{\text{complexed}} &= [I_2]_{w, \text{total}} - [I_2]_{w, \text{free}} \\ &= 0.02832 - 0.000303 \\ &= 0.02802 \text{ mole/liter} \end{aligned}$$

According to equation (10-22), I<sub>2</sub> and KI combine in equimolar concentrations to form the complex. Therefore,

$$[KI]_{\text{complexed}} = [I_2]_{\text{complexed}} = 0.02802 \text{ mole/liter}$$

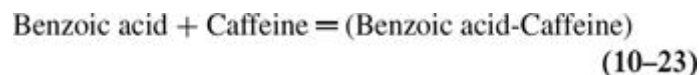
KI is insoluble in carbon disulfide and remains entirely in the aqueous phase. The concentration of *free* KI is thus

$$\begin{aligned} [KI]_{\text{free}} &= [KI]_{\text{total}} - [KI]_{\text{complexed}} \\ &= 0.1250 - 0.02802 \\ &= 0.09698 \text{ mole/liter} \end{aligned}$$

and finally

$$\begin{aligned} K &= \frac{[\text{Complex}]}{[I_2]_{\text{free}} [KI]_{\text{free}}} \\ &= \frac{0.02802}{0.000303 \times 0.09698} = 954 \end{aligned}$$

Higuchi and his associates investigated the complexing action of caffeine, polyvinylpyrrolidone, and polyethylene glycols on a number of acidic drugs, using the partition or distribution method. According to Higuchi and Zuck,<sup>51</sup> the reaction between caffeine and benzoic acid to form the benzoic acid-caffeine complex is



and the stability constant for the reactions at 0°C is

$$K = \frac{[\text{Benzoic acid-Caffeine}]}{[\text{Benzoic acid}][\text{Caffeine}]} = 37.5 \quad (10-24)$$

The results varied somewhat, the value 37.5 being an average stability constant. Guttman and Higuchi<sup>52</sup> later showed that caffeine exists in aqueous solution primarily as a monomer, dimer, and tetramer, which would account in part for the variation in  $K$  as observed by Higuchi and Zuck.

### Solubility Method

According to the solubility method, excess quantities of the drug are placed in well-stoppered containers, together with a solution of the complexing agent in various concentrations, and the bottles are agitated in a constant-temperature bath until equilibrium is attained. Aliquot portions of the supernatant liquid are removed and analyzed.

Higuchi and Lach<sup>53</sup> used the solubility method to investigate the complexation of *p*-aminobenzoic acid (PABA) by caffeine. The results are plotted in Figure 10-12. The point A at which the line crosses the vertical axis is the solubility of

P.212

the drug in water. With the addition of caffeine, the solubility of PABA rises linearly owing to complexation. At point B, the solution is saturated with respect to the complex and to the drug itself. The complex continues to form and to precipitate from the saturated system as more caffeine is added. At point C, all the excess solid PABA has passed into solution and has been converted to the complex. Although the solid drug is exhausted and the solution is no longer saturated, some of the PABA remains uncomplexed in solution, and it combines further with caffeine to form higher complexes such as (PABA-2 caffeine) as shown by the curve at the right of the diagram.

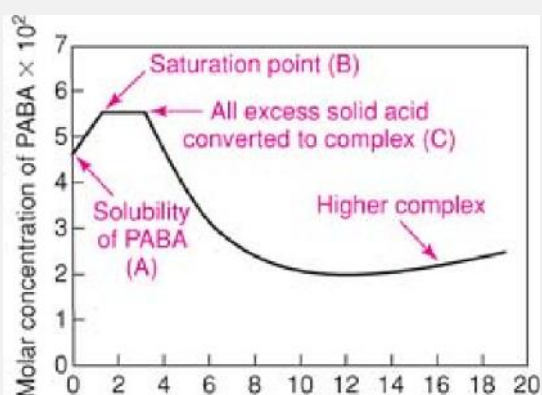


**Fig. 10-12.** The solubility of *para*-aminobenzoic acid (PABA) in the presence of caffeine. (From T. Higuchi and J. L. Lack, *J. Am. Pharm. Assoc. Sci. Ed.* **43**, 525, 1954.)

### Example 10-3

#### Stoichiometric Complex Ratio

The following calculations are made to obtain the stoichiometric ratio of the complex. The concentration of caffeine, corresponding to the plateau BC, equals the concentration of caffeine entering the complex over this range, and the quantity of *p*-aminobenzoic acid entering the complex is obtained from the undissolved solid remaining at point B. It is

computed by subtracting the acid in solution at the saturation point B from the total acid initially added to the mixture, because this is the amount yet undissolved that can form the complex.

The concentration of caffeine in the plateau region is found from Figure 10-12 to be  $1.8 \times 10^{-2}$  mole/liter. The free, undissolved solid PABA is equal to the total acid minus the acid in solution at point B, namely,  $7.3 \times 10^{-2} - 5.5 \times 10^{-2}$ , or  $1.8 \times 10^{-2}$  mole/liter, and the stoichiometric ratio is

$$\frac{\text{Caffeine in complex}}{\text{PABA in complex}} = \frac{1.8 \times 10^{-2}}{1.8 \times 10^{-2}}$$

The complex formation is therefore written as



and the stability constant for this 1:1 complex is

$$K = \frac{[\text{PABA-Caffeine}]}{[\text{PABA}][\text{Caffeine}]} \quad (10-26)$$

$K$  may be computed as follows. The concentration of the complex [PABA-Caffeine] is equal to the total acid concentration at saturation less the solubility [PABA] of the acid in water. The concentration [Caffeine] in the solution at equilibrium is equal to the caffeine added to the system less the concentration that has been converted to the complex. The total acid concentration of saturation is  $4.58 \times 10^{-2}$  mole/liter when no caffeine is added (solubility of PABA) and is  $5.312 \times 10^{-2}$  mole/liter when  $1.00 \times 10^{-2}$  mole/liter of caffeine is added. We have

$$\begin{aligned} [\text{PABA-Caffeine}] &= (5.31 \times 10^{-2}) - (4.58 \times 10^{-2}) \\ &= 0.73 \times 10^{-2} \quad [\text{PABA}] = 4.58 \times 10^{-2} \\ [\text{Caffeine}] &= (1.00 \times 10^{-2}) - (0.73 \times 10^{-2}) = 0.27 \times 10^{-2} \end{aligned}$$

Therefore,

$$K = \frac{[\text{PABA-Caffeine}]}{[\text{PABA}][\text{Caffeine}]} = \frac{0.73 \times 10^{-2}}{(4.58 \times 10^{-2})(0.27 \times 10^{-2})} = 59$$

The stability constants for a number of caffeine complexes obtained principally by the distribution and the solubility methods are given in Table 10-6. Stability constants for a number of other drug complexes were compiled by Higuchi and Connors.<sup>54</sup> Kenley et al.<sup>55</sup> studied water-soluble complexes of various ligands with the antiviral drug acyclovir using the solubility method.

### **Spectroscopy and Charge Transfer Complexation**

Absorption spectroscopy in the visible and ultraviolet regions of the spectrum is commonly used to investigate electron donor-acceptor or charge transfer complexation.<sup>56,57</sup> When iodine is analyzed in a noncomplexing solvent such as  $\text{CCl}_4$ , a curve is obtained with a single peak at about 520 nm. The solution is violet. A solution of iodine in benzene exhibits a maximum shift to 475 nm, and a new peak of considerably higher intensity for the charge-shifted band appears at 300 nm. A solution of iodine in diethyl ether shows a still greater shift to lower wavelength and the appearance of a new maximum. These solutions are red to brown. Their curves are shown in Figure 10-13. In benzene and ether, iodine is the electron acceptor and the organic solvent is the donor; in

P.213

$\text{CCl}_4$ , no complex is formed. The shift toward the ultraviolet region becomes greater as the electron donor solvent becomes a stronger electron-releasing agent. These spectra arise from the transfer of an electron from the donor to the acceptor in close contact in the excited state of the complex. The more easily a donor such as benzene or diethyl ether releases its electron, as measured by its ionization potential, the stronger it is as a donor. Ionization potentials of a series of donors produce a straight line when plotted against the frequency maximum or charge transfer energies ( $1 \text{ nm} = 18.63 \text{ cal/mole}$ ) for solutions of iodine in the donor solvents.<sup>56,57</sup>

<p><b>Table 10-6 Approximate Stability Constants of Some Caffeine Complexes in Water at 30°C</b></p>
--

<b>Compound Complexed with Caffeine</b>	<b>Approximate Stability Constant</b>
Suberic acid	3
Sulfadiazine	7
Picric acid	8
Sulfathiazole	11
<i>o</i> -Phthalic acid	14
Acetylsalicylic acid	15
Benzoic acid (monomer)	18
Salicylic acid	40
<i>p</i> -aminobenzoic acid	48
Butylparaben	50
Benzocaine	59
<i>p</i> -hydroxybenzoic acid	>100

\*Compiled from T. Higuchi et al., J. Am. Pharm. Assoc. Sci. Ed. **42**, 138, 1953; **43**,349, 524, 527, 1954; **45**, 290, 1956; **46**, 32, 1957. Over 500 such complexes with other drugs are recorded by T. Higuchi and K. A. Connors. Phase solubility Techniques, in C. N. Reilley (Ed.), *Advances in Analytical Chemistry and Instrumentation*, Wiley, Vol. 4, New York, 1965, pp. 117–212.

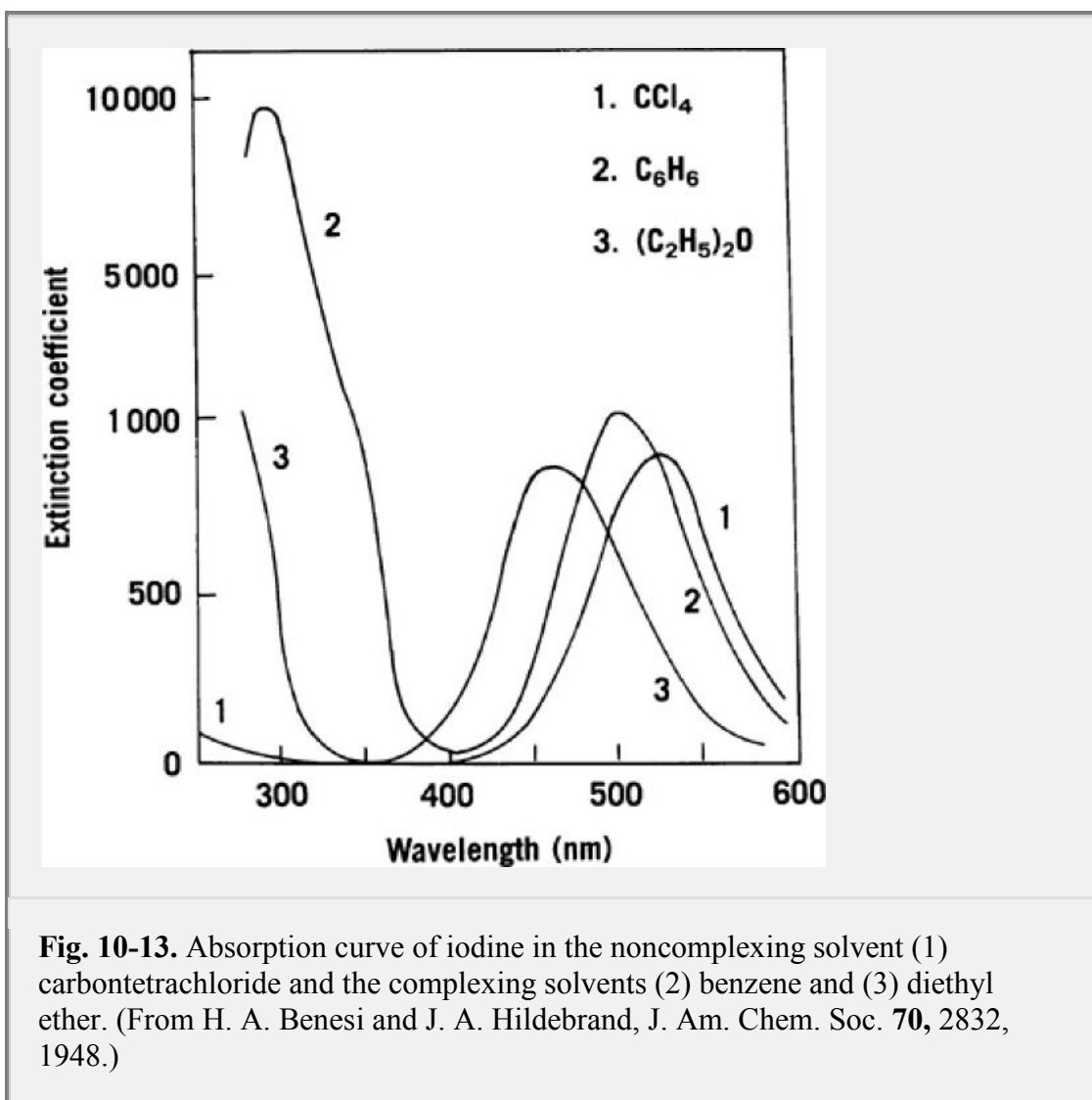
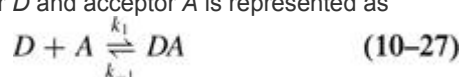


**Fig. 10-13.** Absorption curve of iodine in the noncomplexing solvent (1) carbontetrachloride and the complexing solvents (2) benzene and (3) diethyl ether. (From H. A. Benesi and J. A. Hildebrand, *J. Am. Chem. Soc.* **70**, 2832, 1948.)

The complexation constant,  $K$ , can be obtained by use of visible and ultraviolet spectroscopy. The association between the donor  $D$  and acceptor  $A$  is represented as



where  $K = k_1/k_{-1}$  is the equilibrium constant for complexation (stability constant) and  $k_1$  and  $k_{-1}$  are the interaction rate constants. When two molecules associate according to this scheme and the absorbance  $A$  of the charge transfer band is measured at a definite wavelength,  $K$  is readily obtained from the *Benesi-Hildebrand equation*:

$$\frac{A_0}{A} = \frac{1}{\epsilon} + \frac{1}{K\epsilon} \frac{1}{D_0} \quad (10-28)$$

$A_0$  and  $D_0$  are initial concentrations of the acceptor and donor species, respectively, in mole/liter,  $\epsilon$  is the molar absorptivity of the charge transfer complex at its particular wavelength, and  $K$ , the stability constant, is given in liter/mole or  $M^{-1}$ . A plot of  $A_0/A$  versus  $1/D_0$  results in a straight line with a slope of  $1/(K\epsilon)$  and an intercept of  $1/\epsilon$ , as observed in Figure 10-14.

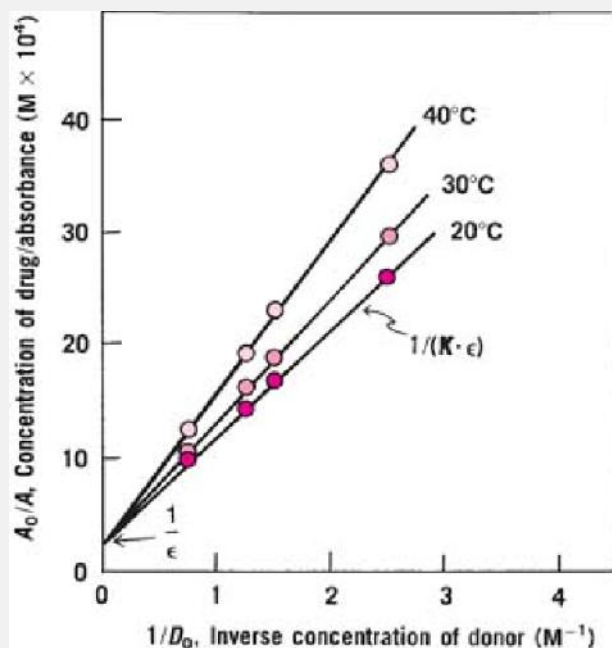


**Fig. 10-14.** A Benesi–Hildebrand plot for obtaining the stability constant,  $K$ , from equation(10-28) for charge transfer complexation. (From M. A. Slifkin, *Biochim. Biophys. Acta* **109**, 617, 1965.)

Borazan et al.<sup>59</sup> investigated the interaction of nucleic acid bases (electron acceptors) with catechol, epinephrine, and isoproterenol (electron donors). Catechols have low ionization potentials and hence a tendency to donate electrons. Charge transfer complexation was evident as demonstrated by ultraviolet absorption measurements. With the assumption of 1:1 complexes, the equilibrium constant,  $K$ , for charge transfer interaction was obtained from Benesi–Hildebrand plots at three or four temperatures, and  $\Delta H^\circ$  was obtained at these same temperatures from the slope of the line as plotted in Figure 10-15. The values of  $K$  and the thermodynamic parameters  $\Delta G^\circ$ ,  $\Delta H^\circ$ , and  $\Delta S^\circ$  are given in Table 10-7.

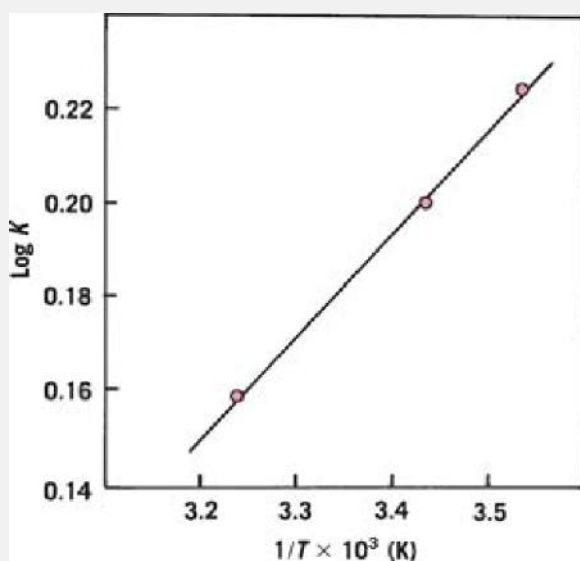


**Fig. 10-15.** Adenine–catechol stability constant for charge transfer complexation measured at various temperatures at a wavelength of 340 nm. (From F. A. Al-Obeidi and H. N. Borazan, *J. Pharm. Sci.* **65**, 892, 1976. With permission.)

P.214

**Table 10-7 Stability Constant,  $K$ , and Thermodynamic Parameters for Charge Transfer Interaction of Nucleic Acid Bases with Catechol in Aqueous Solution\***

Temperature (°C)	$K$ (M)	$\Delta G^\circ$ (cal/mole)	$\Delta H^\circ$ (cal/mole)	$\Delta S^\circ$ (cal/deg mole)
Adenine–catechol				
9	1.69	-294		
18	1.59	-264	-1015	-2.6
37	1.44	-226		
Uracil–catechol				
6	0.49	396		
18	0.38	560	-3564	-14
25	0.32	675		
37	0.26	830		

\*From F. A. Al-Obeidi and H. N. Borazan, *J. Pharm. Sci.* **65**, 892, 1976. With permission.

#### Example 10-4

##### Calculate Molar Absorptivity

When  $A_0/A$  is plotted against  $1/D_0$  for catechol (electron-donor) solutions containing uracil (electron acceptor) in 0.1 N HCl at 6°C, 18°C, 25°C, and 37°C, the four lines were observed to intersect the vertical axis at 0.01041. Total concentration,  $A_0$ , for uracil was  $2 \times 10^{-2}$  M, and  $D_0$  for catechol ranged from 0.3 to 0.8 M. The slopes of the lines determined by the least-squares method were as follows:

6°C	18°C	25°C	37°C
0.02125	0.02738	0.03252	0.04002

Calculate the molar absorptivity and the stability constant,  $K$ . Knowing  $K$  at these four temperatures, how does one proceed to obtain  $\Delta H^\circ$ ,  $\Delta G^\circ$ , and  $\Delta S^\circ$ ?

The intercept, from the Benesi–Hildebrand equation, is the reciprocal of the molar absorptivity, or  $1/0.01041 = 96.1$ . The molar absorptivity,  $\epsilon$ , is a constant for a compound or a complex, independent of temperature or concentration.  $K$  is obtained from the slope of the four curves:

$$(1) 0.02125 = 1/(K \times 96.1); K = 0.49 \text{ M}^{-1}$$

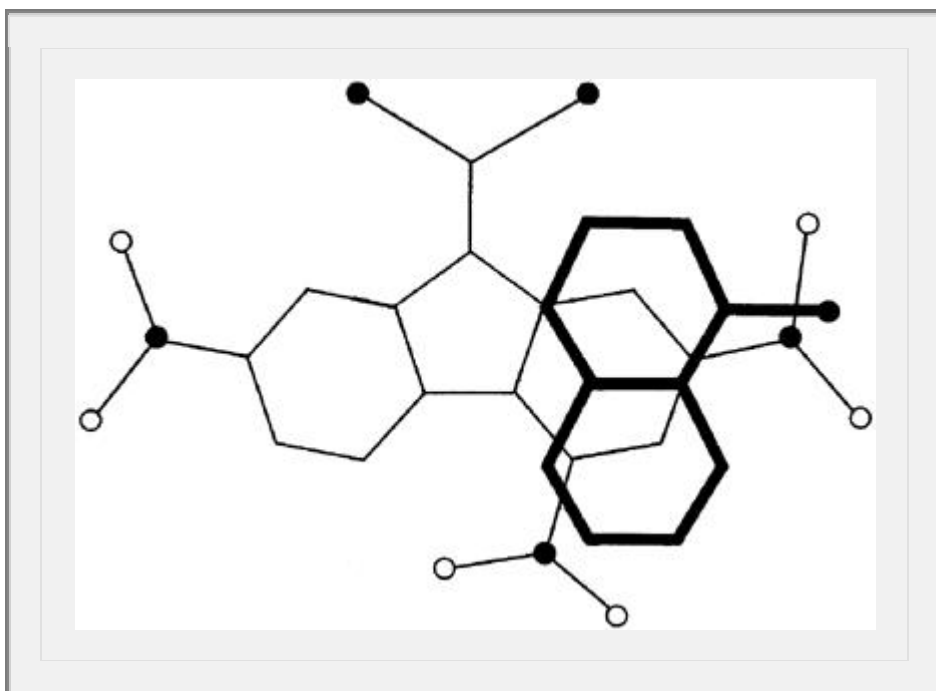
$$(2) 0.02738 = 1/(K \times 96.1); K = 0.38 \text{ M}^{-1}$$

$$(3) 0.03252 = 1/(K \times 96.1); K = 0.32 \text{ M}^{-1}$$

$$(4) 0.04002 = 1/(K \times 96.1); K = 0.26 \text{ M}^{-1}$$

These  $K$  values are then plotted as their logarithms on the vertical axis of a graph against the reciprocal of the four temperatures, converted to kelvin. This is a plot of equation (10-49) and yields  $\Delta H^\circ$  from the slope of the line.  $\Delta G^\circ$  is calculated from  $\log K$  at each of the four temperatures using equation (10-48), in which the temperature,  $T$ , is expressed in kelvin.  $\Delta S^\circ$  is finally obtained using relation:  $\Delta G^\circ = \Delta H^\circ - T\Delta S^\circ$ . The answers to this sample problem are given in Table 10-7.

Webb and Thompson<sup>60</sup> studied the possible role of electron donor–acceptor complexes in drug–receptor binding using quinoline and naphthalene derivatives as model electron donors and a trinitrofluorene derivative as the electron acceptor. The most favorable arrangement for the donor 8-aminoquinoline (heavy lines) and the acceptor 9-dicyanomethylene trinitrofluorene (light lines), as calculated by a quantum chemical method, is shown below:



Filled circles are nitrogen atoms and open circles oxygen atoms. The donor lies above the acceptor molecule at an intermolecular distance of about 3.35 Å and is attached by a binding energy of -5.7 kcal/mole. The negative sign signifies a positive binding force.

### ***Other Methods***

A number of other methods are available for studying the complexation of metal and organic molecular complexes. They include NMR and infrared spectroscopy, polarography, circular dichroism, kinetics, x-ray diffraction, and electron diffraction. Several of these will be discussed briefly in this section.

Complexation of caffeine with L-tryptophan in aqueous solution was investigated by Nishijo et al.<sup>61</sup> using <sup>1</sup>H-NMR spectroscopy. Caffeine interacts with L-tryptophan at a molar ratio of 1:1 by parallel stacking. Complexation is a result of polarization and π - π interactions of the aromatic rings. A possible mode of parallel stacking is shown in Figure 10-16. This study demonstrates that tryptophan, which is presumed to be the binding site in serum albumin for certain drugs, can interact with caffeine even as free amino acid. However,

P.215

caffeine does not interact with other aromatic amino acids such as L-valine or L-leucine.

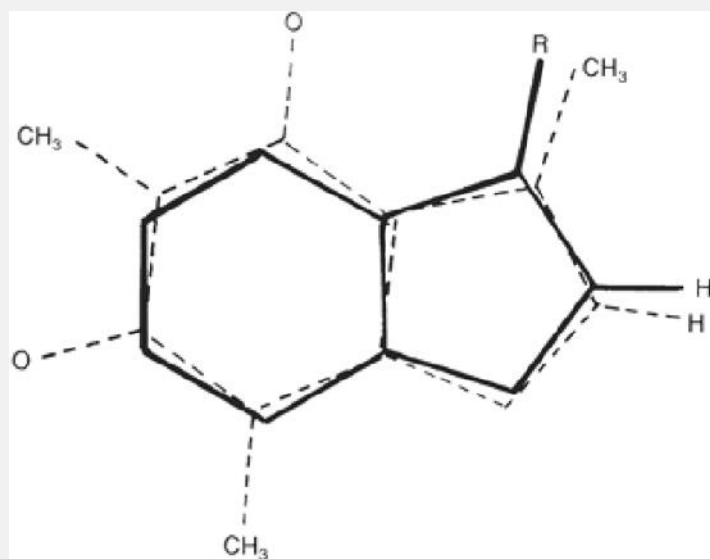


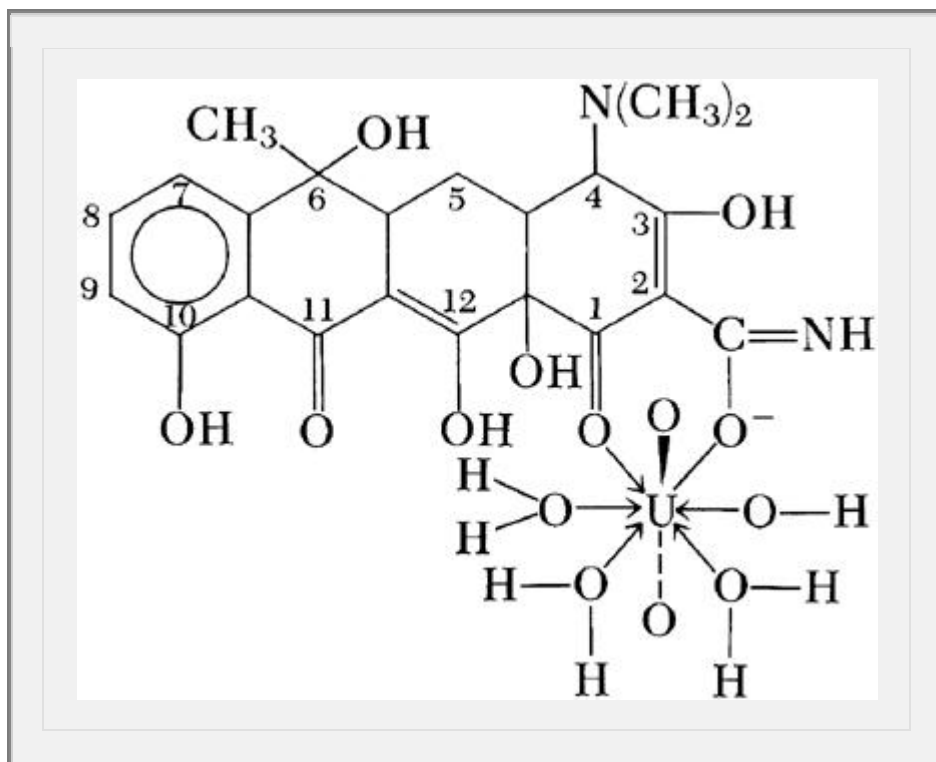
**Fig. 10-16.** Stacking of L-tryptophan (solid line) overlying caffeine (dashed line). The benzene ring of tryptophan is located above the pyrimidine ring of caffeine, and the pyrrole ring of L-tryptophan is above the imidazole ring of caffeine. (From J. Nishijo, I. Yonetami, E. Iwamoto, et al., *J. Pharm. Sci.* **79**, 18, 1990. With permission.)

Borazan and Koumriqian<sup>62</sup> studied the coil-helix transition of polyadenylic acid induced by the binding of the catecholamines norepinephrine and isoproterenol, using circular dichroism. Most mRNA molecules contain regions of polyadenylic acid, which are thought to increase the stability of mRNA and to favor genetic code translation. The change of the circular dichroism spectrum of polyadenylic acid was interpreted as being due to intercalative binding of catecholamines between the stacked adenine bases. These researchers suggested that catecholamines may exert a control mechanism through induction of the coil-to-helix transition of polyadenylic acid, which influences genetic code translation. De Taeye and Zeegers-Huyskens<sup>63</sup> used infrared spectroscopy to investigate the hydrogen-bonded complexes involving polyfunctional bases such as proton donors. This is a very precise technique for determining the thermodynamic parameters involved in hydrogen-bond formation and for characterizing the interaction sites when the molecule has several groups available to form hydrogen-bonded. Caffeine forms hydrogen-bonded complexes with various proton donors: phenol, phenol derivatives, aliphatic alcohols, and water. From the infrared technique, the preferred hydrogen-bonding sites are the carbonyl functions of caffeine. Seventy percent of the complexes are formed at the C=O group at position 6 and 30% of the complexes at the C=O group at position 2 of caffeine. El-Said et al.<sup>64</sup> used conductometric and infrared methods to characterize 1:1 complexes between uranyl acetate and tetracycline. The structure suggested for the uranyl-tetracycline complex is shown below.

### **Key Concept** **Drug-Protein Binding**

The binding of drugs to proteins contained in the body can influence their action in a number of ways. Proteins may (a) facilitate the distribution of drugs throughout the body, (b) inactivate the drug by not enabling a sufficient concentration of free drug to develop at the receptor site, or (c) retard the excretion of a drug. The interaction of a drug with proteins may cause (a) the displacement of body hormones or a coadministered agent, (b) a configurational change in the protein, the structurally altered form of which is capable of binding a coadministered agent, or (c) the formation of a drug-protein complex that itself is biologically active. These topics are discussed in a number of reviews.<sup>65-66</sup> Among the plasma proteins, albumin is the most important owing to its high concentration relative to the other proteins and also to its

ability to bind both acidic and basic drugs. Another plasma protein,  $\alpha_1$ -acid glycoprotein, has been shown to bind numerous drugs; this protein appears to have greater affinity for basic than for acidic drug molecules.



## Protein Binding

A complete analysis of protein binding, including the multiple equilibria that are involved, would go beyond our immediate needs. Therefore, only an abbreviated treatment is given here.

### Binding Equilibria

We write the interaction between a group or free receptor  $P$  in a protein and a drug molecule  $D$  as



The equilibrium constant, disregarding the difference between activities and concentrations, is

$$K = \frac{[PD]}{[P][D_f]} \quad (10-30)$$

or

$$K[P][D_f] = [PD] \quad (10-31)$$

where  $K$  is the association constant,  $[P]$  is the concentration of the protein in terms of free binding sites,  $[D_f]$  is the concentration, usually given in moles, of free drug, sometimes called the ligand, and  $[PD]$  is the concentration of the protein–drug complex.  $K$  varies with temperature and would be better represented as  $K(T)$ ;  $[PD]$ , the symbol for bound drug, is sometimes written as  $[D_b]$ , and  $[D]$ , the free drug, as  $[D_f]$ .

If the total protein concentration is designated as  $[P_t]$ , we can write

$$[P_t] = [P] + [PD]$$

or

$$[P] = [P_t] - [PD] \quad (10-32)$$

Substituting the expression for  $[P]$  from equation (10-32) into (10-31) gives

$$[PD] = K[D_f]([P_t] - [PD]) \quad (10-33)$$

$$[PD] = K[D_f][PD] = K[D_f][P_t] \quad (10-34)$$

$$\frac{[PD]}{P_t} = \frac{K[D_f]}{1 + K[D_f]} \quad (10-35)$$

Let  $r$  be the number of moles of drug bound,  $[PD]$ , per mole of total protein,  $[P_t]$ ; then  $r = [PD]/[P_t]$ , or

$$r = \frac{K[D_f]}{1 + K[D_f]} \quad (10-36)$$

The ratio  $r$  can also be expressed in other units, such as milligrams of drug bound,  $x$ , per gram of protein,  $m$ . Equation (10-36) is one form of the Langmuir adsorption isotherm. Although it is quite useful for expressing protein-binding data, it must not be concluded that obedience to this formula necessarily requires that protein binding be an adsorption phenomenon. Expression (10-36) can be converted to a linear form, convenient for plotting, by inverting it:

$$\frac{1}{r} = \frac{1}{K[D_f]} + 1 \quad (10-37)$$

If  $v$  independent binding sites are available, the expression for  $r$ , equation (10-36), is simply  $v$  times that for a single site, or

$$r = v \frac{K[D_f]}{1 + K[D_f]} \quad (10-38)$$

and equation (10-37) becomes

$$\frac{1}{r} = \frac{1}{vK} \frac{1}{[D_f]} + \frac{1}{v} \quad (10-39)$$

Equation (10-39) produces what is called a *Klotz reciprocal plot*.<sup>67</sup>

An alternative manner of writing equation (10-38) is to rearrange it first to

$$r + rK[D_f] = vK[D_f] \quad (10-40)$$

$$\frac{r}{[D_f]} = vK - rK \quad (10-41)$$

Data presented according to equation (10-41) are known as a *Scatchard plot*.<sup>67,68</sup> The binding of bishydroxycoumarin to human serum albumin is shown as a Scatchard plot in Figure 10-17.

Graphical treatment of data using equation (10-39) heavily weights those experimental points obtained at low concentrations of free drug,  $D$ , and may therefore lead to misinterpretations regarding the protein-binding behavior at high concentrations of free drug. Equation (10-41) does not have this disadvantage and is the method of choice for plotting data. Curvature in these plots usually indicates the existence of more than one type of binding site.

Equations (10-39) and (10-41) cannot be used for the analysis of data if the nature and the amount of protein in the experimental system are unknown. For these situations, Sandberg et al.<sup>69</sup> recommended the use of a slightly modified form of equation (10-41):

$$\frac{[D_b]}{[D_f]} = -K[D_b] + vK[P_t] \quad (10-42)$$

where  $[D_b]$  is the concentration of bound drug. Equation (10-42) is plotted as the ratio  $[D_b]/[D_f]$  versus  $[D_b]$ , and in this way  $K$  is determined from the slope and  $vK[P_t]$  is determined from the intercept.

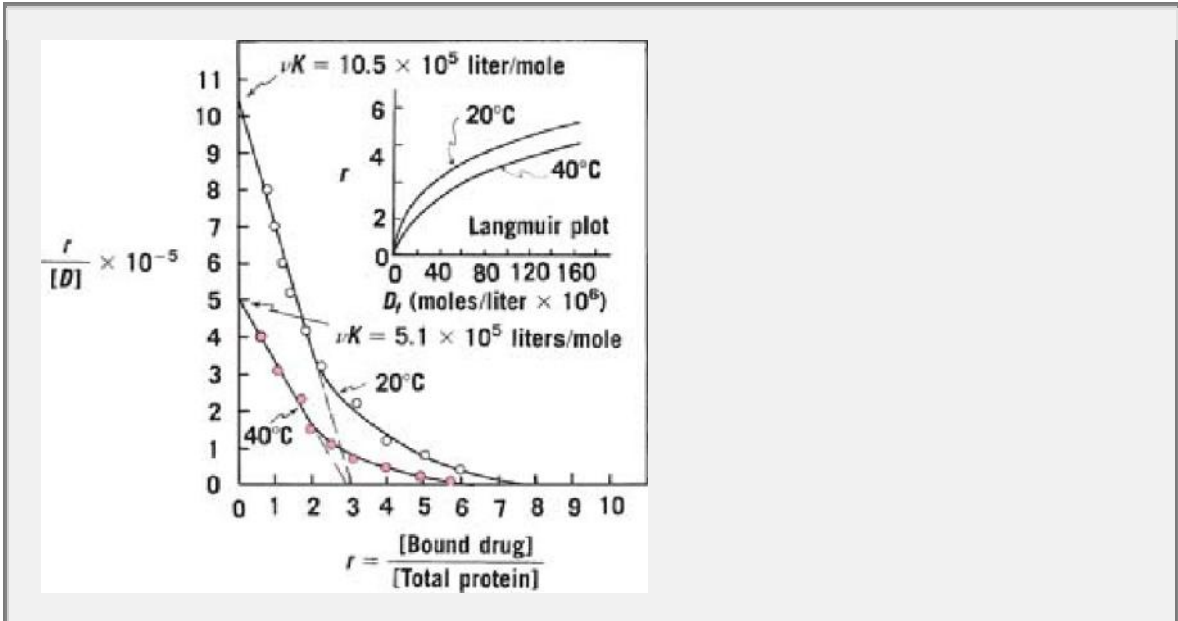


**Fig. 10-17.** A Scatchard plot showing the binding of bishydroxycoumarin to human serum albumin at 20°C and 40°C plotted according to equation(10-41). Extrapolation of the two lines to the horizontal axis, assuming a single class of sites with no electrostatic interaction, gives an approximate value of 3 for  $v$ . (From M. J. Cho, A. G. Mitchell, and M. Pernarowski, *J. Pharm. Sci.* **60**, 196, 1971; **60**, 720, 1971. With permission.) The inset is a Langmuir adsorption isotherm of the binding data plotted according to equation(10-36).

The Scatchard plot yields a straight line when only one class of binding sites is present. Frequently in drug-binding studies,  $n$  classes of sites exist, each class  $i$  having  $v_i$  sites with a unique association constant  $K_i$ . In such a case, the plot of  $r/[D_f]$  versus  $r$  is not linear but exhibits a curvature that suggests the presence of more than one class of binding sites. The data in Figure 10-17 were analyzed in terms of one class of sites for simplification. The plots at 20°C and 40°C clearly show that multiple sites are involved. Blanchard et al.<sup>70</sup> reviewed the case of multiple classes of sites. Equation (10-38) is then written as

$$r = \frac{v_1 K_1 [D_f]}{1 + K_1 [D_f]} + \frac{v_2 K_2 [D_f]}{1 + K_2 [D_f]} + \dots + \frac{v_n K_n [D_f]}{1 + K_n [D_f]} \quad (10-43)$$

or

$$r = \sum_{i=1}^n \frac{v_i K_i [D_f]}{1 + K_i [D_f]} \quad (10-44)$$

As previously noted, only  $v$  and  $K$  need to be evaluated when the sites are all of one class.

When  $n$  classes of sites exist, equations(10-43 and 10-44) can be written as

$$r = \sum_{i=1}^{n-1} \frac{v_i K_i [D_f]}{1 + K_i [D_f]} + v_n K_n [D_f] \quad (10-45)$$

The binding constant,  $K_n$ , in the term on the right is small, indicating extremely weak affinity of the drug for the sites, but this class may have a large number of sites and so be considered unsaturable.

**Equilibrium Dialysis (ED) and Ultrafiltration (UF)**

A number of methods are used to determine the amount of drug bound to a protein. Equilibrium dialysis, ultrafiltration, and electrophoresis are the classic techniques used, and in recent years other methods, such as gel filtration and nuclear magnetic resonance, have been used with satisfactory results. We shall discuss the equilibrium dialysis, ultrafiltration, and kinetic methods.

The equilibrium dialysis procedure was refined by Klotz et al.<sup>71</sup> for studying the complexation between metal ions or small molecules and macromolecules that cannot pass through a semipermeable membrane.

According to the equilibrium dialysis method, the serum albumin (or other protein under investigation) is placed in a Visking cellulose tubing (Visking Corporation, Chicago) or similar dialyzing membrane. The tubes are tied securely and suspended in vessels containing the drug in various concentrations. Ionic strength and sometimes hydrogen ion concentration are adjusted to definite values, and controls and blanks are run to account for the adsorption of the drug and the protein on the membrane.

If binding occurs, the drug concentration in the sac containing the protein is greater at equilibrium than the concentration of drug in the vessel outside the sac. Samples are removed and analyzed to obtain the concentrations of free and complexed drug.

Equilibrium dialysis is the classic technique for protein binding and remains the most popular method. Some potential errors associated with this technique are the possible binding of drug to the membrane, transfer of substantial amounts of drug from the plasma to the buffer side of the membrane, and osmotic volume shifts of fluid to the plasma side. Tozer et al.<sup>72</sup> developed mathematical equations to calculate and correct for the magnitude of fluid shifts. Briggs et al.<sup>73</sup> proposed a modified equilibrium dialysis technique to minimize experimental errors for the determination of low levels of ligand or small molecules.

Ultrafiltration methods are perhaps more convenient for the routine determination because they are less time-consuming. The ultrafiltration method is similar to equilibrium dialysis in that macromolecules such as serum albumin are separated from small drug molecules. Hydraulic pressure or centrifugation is used in ultrafiltration to force the solvent and the small molecules, unbound drug, through the membrane while preventing the passage of the drug bound to the protein. This ultrafiltrate is then analyzed by spectrophotometry or other suitable technique.

The concentration of the drug that is free and unbound,  $D_f$ , is obtained by use of the Beer's law equation:

$$A = \epsilon bc \quad (10-46)$$

where  $A$  is the spectrophotometric absorbance (dimensionless),  $\epsilon$  is the molar absorptivity, determined independently for each drug,  $c$  ( $D_f$  in binding studies) is the concentration of the free drug in the ultrafiltrate in moles/liter, and  $b$  is the optical path length of the spectrophotometer cell, ordinarily 1 cm. The following example outlines the steps involved in calculating the Scatchard  $r$  value and the percentage of drug bound.

### Example 10-5

#### Binding to Human Serum Albumin

The binding of sulfamethoxyipyridazine to human serum albumin was studied at 25°C, pH 7.4, using the ultrafiltration technique. The concentration of the drug under study,  $[D_t]$ , is  $3.24 \times 10^{-5}$  mole/liter and the human serum albumin concentration,  $[P]$ , is  $1.0 \times 10^{-4}$  mole/liter. After equilibration the ultrafiltrate has an absorbance,  $A$ , of 0.559 at 540 nm in a cell whose optical path length,  $b$ , is 1 cm. The molar absorptivity,  $\epsilon$ , of the drug is  $5.6 \times 10^4$  liter/mole cm.

Calculate the Scatchard  $r$  value and the percentage of drug bound.

The concentration of free (unbound) drug,  $[D_f]$ , is given by

$$[D_f] = \frac{A}{b\epsilon} = \frac{0.559}{(5.6 \times 10^4)1} = 0.99 \times 10^{-5} \text{ mole/liter}$$

The concentration of bound drug,  $[D_b]$ , is given by

$$\begin{aligned} [D_b] &= [D_t] - [D_f] \\ &= (3.24 \times 10^{-5}) - (0.99 \times 10^{-5}) \\ &= 2.25 \times 10^{-5} \text{ mole/liter} \end{aligned}$$

The  $r$  value is

$$r = \frac{[D_b]}{[P_t]} = \frac{2.25 \times 10^{-5}}{1.0 \times 10^{-4}} = 0.225$$

The percentage of bound drug is  $[D_b]/[D_t] \times 100 = 69\%$ .

A potential error in ultrafiltration techniques may result from the drug binding to the membrane. The choice between ultrafiltration and equilibrium dialysis methods depends on P.218

the characteristics of the drug. The two techniques have been compared in several protein-binding studies.<sup>74,75,76</sup>

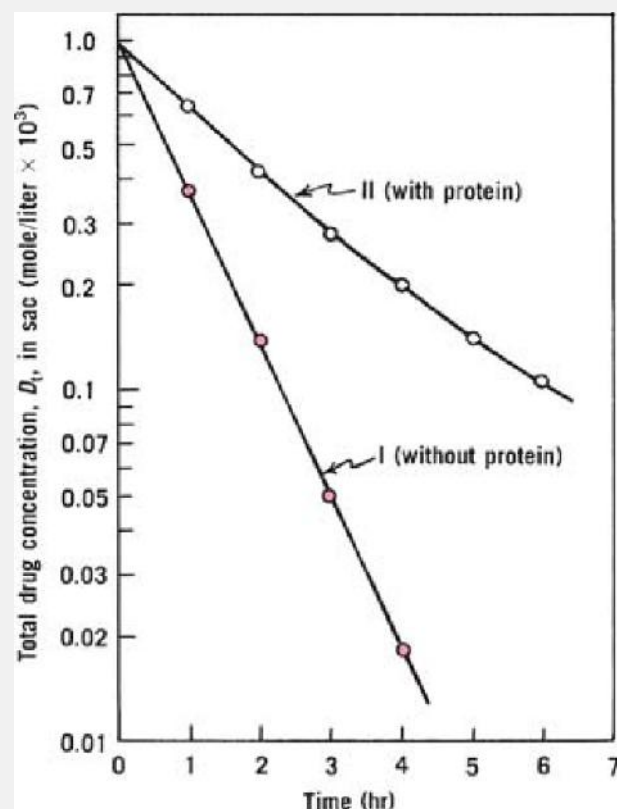


**Fig. 10-18.** The dynamic dialysis plot for determining the concentration of bound drug in a protein solution (From M. C. Meyer and D. E. Guttman, *J. Pharm. Sci.* **57**, 1627, 1968. With permission).

### Key Concept

#### Protein Binding

Protein binding (PB) plays an important role in the pharmacokinetics and pharmacodynamics of a drug. The extent of PB in the plasma or tissue controls the volume of distribution and affects both hepatic and renal clearance. In many cases, the free drug concentration, rather than the total concentration in plasma, is correlated to the effect. Drug displacement from drug-protein complex can occur by direct competition of two drugs for the same binding site and is important with drugs that are highly bound (>95%), for which a small displacement of bound drug can greatly increase the free drug concentration in the plasma. In order to measure free fraction or PB of a drug, ultrafiltration (UF), ultracentrifugation, equilibrium dialysis (ED), chromatography, spectrophotometry, electrophoresis, etc. have been used. Essential methodologic aspects of PB study include the selection of assay procedures, devices, and materials. The most commonly used method for PB measurement is ED, which

is believed to be less susceptible to experimental artifacts. However, it is time consuming and is not suitable for unstable compounds because it requires substantial equilibration time (3–24 hr) depending on drugs, membrane materials, and devices. Many researchers have used UF centrifugal devices for PB measurement. UF is a simple and rapid method in which centrifugation forces the buffer containing free drugs through the size exclusion membrane and achieves a fast separation of free from protein-bound drug. However, the major disadvantage of this method is nonspecific binding of drugs on filter membranes and plastic devices. When the drug binds extensively to the filtration membrane, the ultrafiltrate concentration may deviate from the true free concentration. (From K.-J. Lee, R. Mower, T. Hollenbeck, J. Castelo, N. Johnson, P. Gordon, P. J. Sinko, K. Holme, and Y.-H. Lee, *Pharm. Res.* **20**, 1015, 2003. With permission.)

### Dynamic Dialysis

Meyer and Guttman<sup>77</sup> developed a kinetic method for determining the concentrations of bound drug in a protein solution. The method has found favor in recent years because it is relatively rapid, economical in terms of the amount of protein required, and readily applied to the study of competitive inhibition of protein binding. It is discussed here in some detail. The method, known as *dynamic dialysis*, is based on the rate of disappearance of drug from a dialysis cell that is proportional to the concentration of unbound drug. The apparatus consists of a 400-mL jacketed (temperature-controlled) beaker into which 200 mL of buffer solution is placed. A cellophane dialysis bag containing 7 mL of drug or drug–protein solution is suspended in the buffer solution. Both solutions are stirred continuously. Samples of solution external to the dialysis sac are removed periodically and analyzed spectrophotometrically, and an equivalent amount of buffer solution is returned to the external solution. The dialysis process follows the rate law

$$\frac{-d[D_t]}{dt} = k[D_t] \quad (10-47)$$

where  $[D_t]$  is the total drug concentration,  $[D_f]$  is the concentration of free or unbound drug in the dialysis sac,  $-d[D_t]/dt$  is the rate of loss of drug from the sac, and  $k$  is the first-order rate constant (see Chapter 13) representative of the diffusion process. The factor  $k$  can also be referred to as the apparent permeability rate constant for the escape of drug from the sac. The concentration of unbound drug,  $[D_f]$ , in the sac (protein compartment) at a total drug concentration  $[D_t]$  is calculated using equation (10-45), knowing  $k$  and the rate  $-d[D_t]/dt$  at a particular drug concentration,  $[D_t]$ . The rate constant,  $k$ , is obtained from the slope of a semilogarithmic plot of  $[D_t]$  versus time when the experiment is conducted in the absence of the protein.

Figure 10-18 illustrates the type of kinetic plot that can be obtained with this system. Note that in the presence of protein, curve II, the rate of loss of drug from the dialysis sac is slowed compared with the rate in the absence of protein, curve I. To solve equation (10-47) for free drug concentration,  $[D_f]$ , it is necessary to determine the slope of curve II at various points in time. This is not done graphically, but instead it is accurately accomplished by first fitting the time-course data to a suitable empirical equation, such as the following, using a computer.

$$[D_t] = C_1 e^{-C_2 t} + C_3 e^{-C_4 t} + C_5 e^{-C_6 t} \quad (10-48)$$

The computer fitting provides estimates of  $C_1$  through  $C_6$ . The values for  $d[D_t]/dt$  can then be computed from equation (10-49), which represents the first derivative of equation (10-48):

$$-\frac{d[D_t]}{dt} = C_1 C_2 e^{-C_2 t} + C_3 C_4 e^{-C_4 t} + C_5 C_6 e^{-C_6 t} \quad (10-49)$$

Finally, once we have a series of  $[D_t]$  values computed from equations (10-49) and (10-47) corresponding to experimentally determined values of  $[D_t]$  at each time  $t$ , we can proceed to calculate the various terms for the Scatchard plot.

#### Example 10-6\*

##### Calculate Scatchard Values

Assume that the kinetic data illustrated in Figure 10-18 were obtained under the following conditions: initial drug concentration,  $[D_{t0}]$ , is  $1 \times 10^{-3}$  mole/liter and protein concentration is  $1 \times 10^{-3}$  mole/liter. Also assume that the first-order rate constant,  $k$ , for the control (curve I) was

determined to be  $1.0 \text{ hr}^{-1}$  and that fitting of curve II to equation (10-48) resulted in the following empirical constants:  $C_1 = 5 \times 10^{-4} \text{ mole/liter}$ ,  $C_2 = 0.6 \text{ hr}^{-1}$ ,  $C_3 = 3 \times 10^{-4} \text{ mole/liter}$ ,  $C_4 = 0.4 \text{ hr}^{-1}$ ,  $C_5 = 2 \times 10^{-4} \text{ mole/liter}$ , and  $C_6 = 0.2 \text{ hr}^{-1}$ .

Calculate the Scatchard values (the Scatchard plot was discussed in the previous section) for  $r$  and  $r/[D_f]$  if, during the dialysis in the presence of protein, the experimentally determined value for  $[D_f]$  was  $4.2 \times 10^{-4} \text{ mole/liter}$  at 2 hr. Here,  $r = [D_b]/P_t$ , where  $[D_b]$  is drug bound and  $P_t$  is total protein concentration. We have  
Using equation (10-49),

$$\begin{aligned} -\frac{d[D_f]}{dt} &= k[D_f] \\ &= (5 \times 10^{-4})(0.6)e^{-0.6(2)} + (3 \times 10^{-4})(0.4)e^{-0.4(2)} \\ &\quad + (2 \times 10^{-4})(0.2)e^{-0.2(2)} \end{aligned}$$

where the (2) in the exponent stands for 2 hr. Thus,

$$[D_f]_{2 \text{ hr}} = \frac{1.7 \times 10^{-4} \text{ mole/liter hr}^{-1}}{1.0 \text{ hr}^{-1}} = 1.7 \times 10^{-4} \text{ mole/liter}$$

It follows that at 2 hr,

$$\begin{aligned} [D_b] &= [D_f] - [D_f] \\ &= 4.2 \times 10^{-4} \text{ mole/liter} - 1.7 \times 10^{-4} \text{ mole/liter} \\ &= 2.5 \times 10^{-4} \text{ mole/liter} \\ r &= [D_b]/[P_t] = (2.5 \times 10^{-4})/(1 \times 10^{-3}) = 0.25 \\ (r)/[D_f] &= (0.25)/(1.7 \times 10^{-4}) = 1.47 \times 10^3 \text{ liter/mole} \end{aligned}$$

Additional points for the Scatchard plot would be obtained in a similar fashion, using the data obtained at various points throughout the dialysis. Accordingly, this series of calculations permits one to prepare a Scatchard plot (see Fig. 10-17).

P.219

Judis78 investigated the binding of phenol and phenol derivatives by whole human serum using the dynamic dialysis technique and presented the results in the form of Scatchard plots.

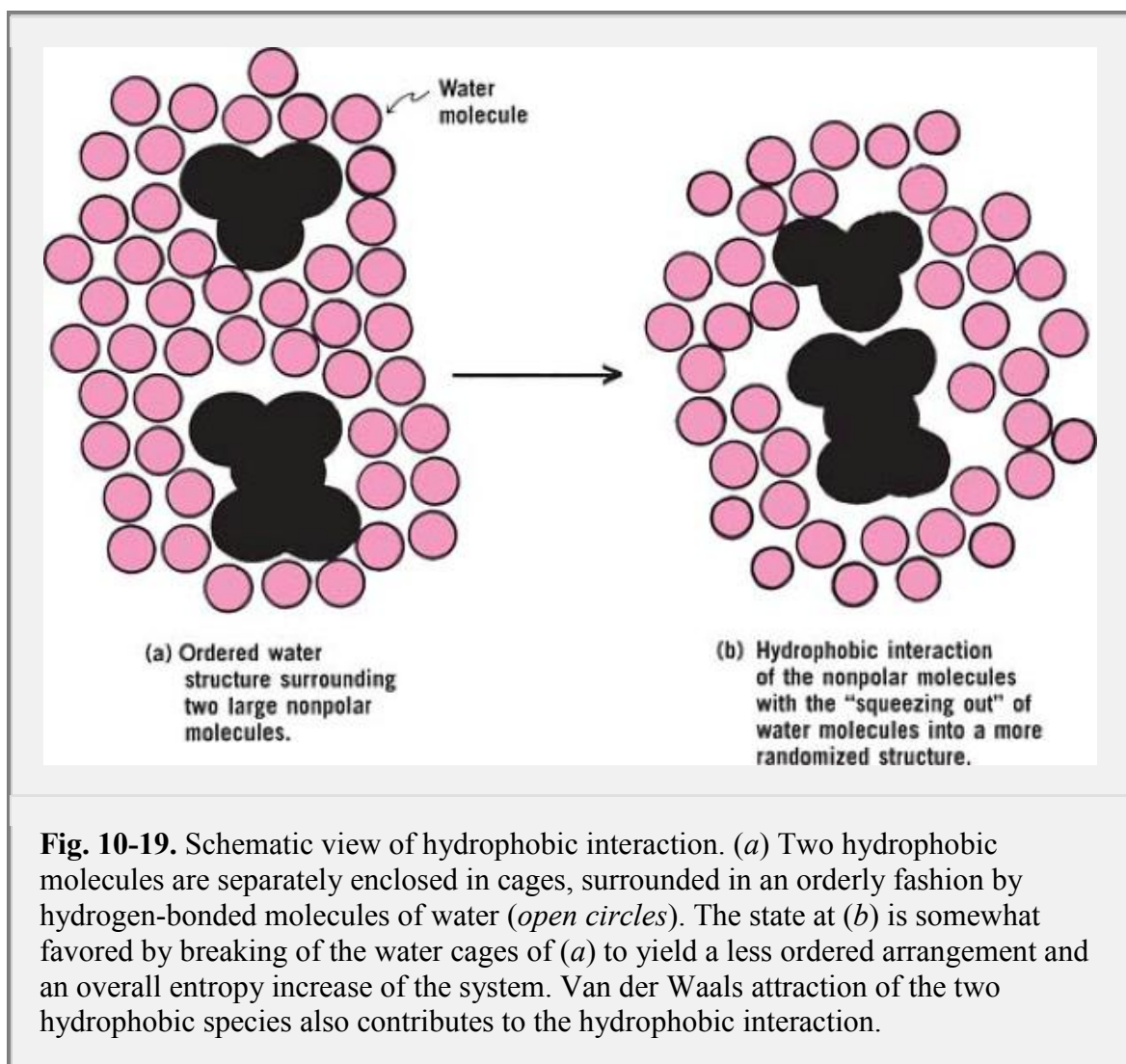


**Fig. 10-19.** Schematic view of hydrophobic interaction. (a) Two hydrophobic molecules are separately enclosed in cages, surrounded in an orderly fashion by hydrogen-bonded molecules of water (*open circles*). The state at (b) is somewhat favored by breaking of the water cages of (a) to yield a less ordered arrangement and an overall entropy increase of the system. Van der Waals attraction of the two hydrophobic species also contributes to the hydrophobic interaction.

### **Hydrophobic Interaction**

Hydrophobic “bonding,” first proposed by Kauzmann,<sup>79</sup> is actually not bond formation at all but rather the tendency of hydrophobic molecules or hydrophobic parts of molecules to avoid water because they are not readily accommodated in the hydrogen-bonding structure of water. Large hydrophobic species such as proteins avoid the water molecules in an aqueous solution insofar as possible by associating into micellelike structures (Chapter 15) with the nonpolar portions in contact in the inner regions of the “micelles,” the polar ends facing the water molecules. This attraction of hydrophobic species, resulting from their unwelcome reception in water, is known as hydrophobic bonding, or, better, *hydrophobic interaction*. It involves van der Waals forces, hydrogen bonding of water molecules in a three-dimensional structure, and other interactions. Hydrophobic interaction is favored thermodynamically because of an increased disorder or entropy of the water molecules that accompanies the association of the nonpolar molecules, which squeeze out the water. Globular proteins are thought to maintain their ball-like structure in water because of the hydrophobic effect. Hydrophobic interaction is depicted in Figure 10-19.

Nagwekar and Kostenbauder<sup>80</sup> studied hydrophobic effects in drug binding, using as a model of the protein a copolymer of vinylpyridine and vinylpyrrolidone. Kristiansen et al.<sup>81</sup> studied the effects of organic solvents in decreasing complex formation between small organic molecules in aqueous solution. They attributed the interactions of the organic species to a significant contribution by both hydrophobic bonding and the unique effects of the water structure. They suggested that some nonclassic “donor–acceptor” mechanism may be operating to lend stability to the complexes formed.

Feldman and Gibaldi<sup>82</sup> studied the effects of urea, methylurea, and 1,3-dimethylurea on the solubility of benzoic and salicylic acids in aqueous solution. They concluded that the enhancement of solubility by urea and its derivatives was a result of hydrophobic bonding rather than complexation. Urea broke up the hydrogen-bonded water clusters surrounding the nonpolar solute molecules, increasing the entropy of the system and producing a driving force for solubilization of benzoic and salicylic acids. It may be possible that the ureas formed channel complexes with these aromatic acids as shown in Figure 10-3 *a*, *b*, and *c*.

The interaction of drugs with proteins in the body may involve hydrophobic bonding at least in part, and this force in turn may affect the metabolism, excretion, and biologic activity of a drug.

### **Self-Association**

Some drug molecules may self-associate to form dimers, trimers, or aggregates of larger sizes. A high degree of association may lead to formation of micelles, depending on the nature of the molecule (Chapter 16). Doxorubicin forms dimers, the process being influenced by buffer composition and ionic strength. The formation of tetramers is favored by hydrophobic stacking aggregation.<sup>83</sup> Self-association may affect solubility, diffusion, transport through membranes, and therapeutic action. Insulin shows concentration-dependent self-association, which leads to complications in the treatment of diabetes. Aggregation is of particular importance in long-term insulin devices, where insulin crystals have been observed. The initial step of insulin self-association is a hydrophobic interaction of the monomers to form dimers, which further associate into larger aggregates. The process is favored at higher concentrations of insulin.<sup>84</sup> Addition of urea at nontoxic concentrations (1.0–3 mg/mL) has been shown to inhibit the self-association of insulin. Urea breaks up the “icebergs” in liquid water and associates with structured water by hydrogen bonding, taking an active part in the formation of a more open “lattice” structure.<sup>85</sup> Sodium salicylate improves the rectal absorption of a number of drugs, all of them exhibiting self-association. Touitou and Fisher<sup>86</sup> chose methylene blue as a model for studying the effect of sodium salicylate on molecules that self-associate by a process of stacking. Methylene blue is a planar aromatic dye that forms dimers, trimers, and higher aggregates in aqueous solution. The workers found that sodium salicylate prevents the self-association of methylene blue. The inhibition of aggregation of porcine insulin by sodium salicylate results in a 7875-fold increase in solubility.<sup>87</sup> Commercial heparin samples tend to aggregate in storage depending on factors such as temperature and time in storage.<sup>88</sup>

### **Factors Affecting Complexation and Protein Binding**

Kenley et al.<sup>55</sup> investigated the role of hydrophobicity in the formation of water-soluble complexes. The logarithm of the ligand partition coefficient between octanol and water was chosen as a measure of hydrophobicity of the ligand. The authors found a significant correlation between the stability constant of the complexes and the hydrophobicity of the ligands. Electrostatic forces were not considered as important because all compounds studied were uncharged under the conditions investigated. Donor–acceptor properties expressed in terms of orbital energies (from quantum chemical calculations) and relative donor–acceptor strengths correlated poorly with the formation constants of the complex. It was suggested that ligand hydrophobicity is the main contribution to the formation of water-soluble complexes. Coulson and Smith<sup>89</sup> found that the more hydrophobic chlorobiocin analogues showed the highest percentage of drug bound to human serum albumin. These workers suggested that chlorobiocin analogues bind to human albumin at the same site as warfarin. This site consists of two noncoplanar hydrophobic areas and a cationic group. Warfarin, an anticoagulant, serves as a model drug in protein-binding studies because it is extensively but weakly bound. Thus, many drugs are able to compete with and displace warfarin from its binding sites. The displacement may result in a sudden increase of the free (unbound) fraction in plasma, leading to toxicity, because only the free fraction of a drug is pharmacologically active. Diana et al.<sup>90</sup> investigated the displacement of warfarin by nonsteroidal anti-inflammatory drugs. Table 10-8 shows the variation of the stability constant,  $K$ , and the number of binding sites,  $n$ , of the complex albumin–warfarin after addition of competing drugs. Azapropazone

markedly decreases the  $K$  value, suggesting that both drugs, warfarin and azapropazone, compete for the same binding site on albumin. Phenylbutazone also competes strongly for the binding site on albumin. Conversely, tolmetin may increase  $K$ , as suggested by the authors, by a conformational change in the albumin molecule that favors warfarin binding. The other drugs (see Table 10-8) decrease the  $K$  value of warfarin to a lesser extent, indicating that they do not share exclusively the same binding site as that of warfarin.

Plaizier-Vercammen<sup>91</sup> studied the effect of polar organic solvents on the binding of salicylic acid to povidone. He

P.221

found that in water–ethanol and water–propylene glycol mixtures, the stability constant of the complex decreased as the dielectric constant of the medium was lowered. Such a dependence was attributed to hydrophobic interaction and can be explained as follows. Lowering the dielectric constant decreases polarity of the aqueous medium. Because most drugs are less polar than water, their *affinity to the medium increases* when the dielectric constant decreases. As a result, the binding to the macromolecule is reduced.

**Table 10-8 Binding Parameters ( $\pm$  Standard Deviation) for Warfarin in the Presence of Displacing Drugs\***

Competing Drug	Racemic Warfarin	
	$n$	$K \times 10^{-5} \text{ M}^{-1}$
None	1.1 $\pm$ 0.0	6.1 $\pm$ 0.2
Azapropazone	1.4 $\pm$ 0.1	0.19 $\pm$ 0.02
Phenylbutazone	1.3 $\pm$ 0.2	0.33 $\pm$ 0.06
Naproxen	0.7 $\pm$ 0.0	2.4 $\pm$ 0.2
Ibuprofen	1.2 $\pm$ 0.2	3.1 $\pm$ 0.4
Mefenamic acid	0.9 $\pm$ 0.0	3.4 $\pm$ 0.2
Tolmetin	0.8 $\pm$ 0.0	12.6 $\pm$ 0.6

\*From F. J. Diana, K. Veronich, and A. L. Kapoor, *J. Pharm. Sci.* **78**, 195, 1989. With permission.

Protein binding has been related to the solubility parameter  $\delta$  of drugs. Bustamante and Selles<sup>92</sup> found that the percentage of drug bound to albumin in a series of sulfonamides showed a maximum at  $\Delta = 12.33 \text{ cal}^{1/2} \text{ cm}^{-3/2}$ . This value closely corresponds to the  $\delta$  value of the postulated binding site on albumin for sulfonamides and suggests that the closer the solubility parameter of a drug to the  $\delta$  value of its binding site, the greater is the binding.

## Chapter Summary

Complexation is widely used in the pharmaceutical sciences to improve properties such as solubility. The three classes of complexes or coordination compounds were discussed in the context to identify pharmaceutically relevant examples. The physical properties of chelates and what differentiates them from organic molecular complexes were also described. The types of forces that hold together organic molecular complexes also play an important role in determining the function and use of complexes in the pharmaceutical sciences. One widely used complex system, the cyclodextrins, was described in detail with respect to pharmaceutical applications. The stoichiometry and stability of complexes was described as well as methods of analysis to determine their strengths and weaknesses. Protein binding is important for many drug substances. The ways in which protein binding could influence drug action were discussed. Also, methods such as the equilibrium dialysis and ultrafiltration were described for determining protein binding.

Practice problems for this chapter can be found at [thePoint.lww.com/Sinko6e](http://thePoint.lww.com/Sinko6e).

## References

1. L. Pauling, *The Nature of the Chemical Bond*, Cornell University Press, Ithaca, New York, 1940, p. 81.
2. A. Werner, *Vjschr. naturf. Ges. Zurich*, **36**, 129, 1891.
3. P. Mohanakrishnan, C. F. Chignell, and R. H. Cox, *J. Pharm. Sci.* **74**, 61, 1985.
4. J. E. Whitaker and A. M. Hoyt, Jr., *J. Pharm. Sci.* **73**, 1184, 1984.
5. A. E. Martell and M. Calvin, *Chemistry of the Metal Chelate Compounds*, Prentice Hall, New York, 1952.
6. L. B. Clapp, in J. R. Bailar, Jr. (Ed.), *The Chemistry of the Coordination Compounds*, Reinhold, New York, 1956, Chapter 17.
7. G. Canti, A. Scozzafava, G. Ciciani, and G. Renzi, *J. Pharm. Sci.* **69**, 1220, 1980.
8. F. J. Bullock, in M. Florkin and E. H. Stotz (Eds.), *Comprehensive Biochemistry*, Elsevier, New York, 1967, pp. 82–85.
9. J. Buxeraud, A. C. Absil, and C. Raby, *J. Pharm. Sci.* **73**, 1687, 1984.
10. T. Higuchi and J. L. Lach, *J. Am. Pharm. Assoc. Sci. Ed.* **43**, 349, 525, 527, 1954; T. Higuchi and D. A. Zuck, *J. Am. Pharm. Assoc. Sci. Ed.* **42**, 132, 1953.
11. T. Higuchi and L. Lachman, *J. Am. Pharm. Assoc. Sci. Ed.* **44**, 521, 1955; L. Lachman, L. J. Ravin, and T. Higuchi, *J. Am. Pharm. Assoc. Sci. Ed.* **45**, 290, 1956; L. Lachman and T. Higuchi, *J. Am. Pharm. Assoc. Sci. Ed.* **46**, 32, 1957.
12. T. Higuchi and I. H. Pitman, *J. Pharm. Sci.* **62**, 55, 1973.
13. P. York and A. Saleh, *J. Pharm. Sci.* **65**, 493, 1976.
14. A. Marcus, *Drug Cosmet. Ind.* **79**, 456, 1956.
15. J. A. Plaizier-Vercammen and R. E. De Nève, *J. Pharm. Sci.* **70**, 1252, 1981; J. A. Plaizier-Vercammen, *J. Pharm. Sci.* **76**, 817, 1987.
16. K. H. Frömming, W. Ditter, and D. Horn, *J. Pharm. Sci.* **70**, 738, 1981.
17. D. S. Hayward, R. A. Kenley, and D. R. Jenke, *Int. J. Pharm.* **59**, 245, 1990.
18. T. Hosono, S. Tsuchiya, and H. Matsumaru, *J. Pharm. Sci.* **69**, 824, 1980.
19. B. J. Forman and L. T. Grady, *J. Pharm. Sci.* **58**, 1262, 1969.
20. H. van Olphen, *Introduction to Clay Colloid Chemistry*, 2nd Ed., Wiley, New York, 1977, pp. 66–68.
21. *Merck Index*, 11th Ed., Merck, Rahway, N.J., 1989, p. 365.
22. J. A. A. Ketelaar, *Chemical Constitution*, Elsevier, New York, 1958, p. 365.
23. H. M. Powell and D. E. Palin, *J. Chem. Soc.* **208**, 1947; *J. Chem. Soc.* **61**, 571, 815, 1948; *J. Chem. Soc.* **298**, 300, 468, 1950; *J. Chem. Soc.* 2658, 1954.
24. (a) S. G. Frank, *J. Pharm. Sci.* **64**, 1585, 1975; (b) M. E. Davis and M. E. Brewster, *Nat. Rev. Drug Discov.* **3**, 1023, 2004.
25. K. Cabrera and G. Schwinn, *Am. Lab.* **22**, 22, 24, 26, 28, 1990.

26. D. Duchêne and D. Wouessidjewe, *Pharm. Tech.* **14**(6), 26, 28, 32, 34, 1990; **14**(8), 22, 24, 26, 28, 30, 1990.
27. O. Beckers, J. H. Beijnen, E. H. G. Bramel, M. Otagiri, A. Bult, and W. J. M. Underberg, *Int. J. Pharm.* **52**, 239, 1989.
28. T. Bakensfield, B. W. Müller, M. Wiese, and J. Seydel, *Pharm. Res.* **7**, 484, 1990.
29. J. L. Lach and J. Cohen, *J. Pharm. Sci.* **52**, 137, 1963; W. A. Pauli and J. Lach, *J. Pharm. Sci.* **54**, 1945, 1965; J. Lach and W. A. Pauli, *J. Pharm. Sci.* **55**, 32, 1966.
30. D. Amdidouche, H. Darrouzet, D. Duchêne, and M.-C. Poelman, *Int. J. Pharm.* **54**, 175, 1989.
31. M. A. Hassan, M. S. Suleiman, and N. M. Najib, *Int. J. Pharm.* **58**, 19, 1990.
32. F. Kedzierewicz, M. Hoffman, and P. Maincent, *Int. J. Pharm.* **58**, 22, 1990.
33. M. E. Brewster, K. S. Estes, and N. Bodor, *Int. J. Pharm.* **59**, 231, 1990; M. E. Brewster, K. S. Estes, T. Loftsson, R. Perchalski, H. Derendorf, G. Mullersman, and N. Bodor, *J. Pharm. Sci.* **77**, 981, 1988.
34. A. R. Green and J. K. Guillory, *J. Pharm. Sci.* **78**, 427, 1989.
35. B. W. Müller and U. Brauns, *J. Pharm. Sci.* **75**, 571, 1986.
36. J. Pitha, E. J. Anaissie, and K. Uekama, *J. Pharm. Sci.* **76**, 788, 1987.
37. Y. Horiuchi, F. Hiriyama, and K. Uekama, *J. Pharm. Sci.* **79**, 128, 1990.
38. F. Hirayama, N. Hirashima, K. Abe, K. Uekama, T. Ijitsu, and M. Ueno, *J. Pharm. Sci.* **77**, 233, 1988.
39. F. M. Andersen, H. Bungaard, and H. B. Mengel, *Int. J. Pharm.* **21**, 51, 1984.
40. K. A. Connors, in *A Textbook of Pharmaceutical Analysis*, Wiley, New York, 1982, Chapter 4; K. A. Connors, *Binding Constants*, Wiley, New York, 1987.
41. P. Job, *Ann. Chim.* **9**, 113, 1928.
42. A. E. Martell and M. Calvin, *Chemistry of the Metal Chelate Compounds*, Prentice Hall, New York, 1952, p. 98.
43. M. E. Bent and C. L. French, *J. Am. Chem. Soc.* **63**, 568, 1941; R. E. Moore and R. C. Anderson, *J. Am. Chem. Soc.* **67**, 168, 1945.
44. W. C. Vosburgh, et al., *J. Am. Chem. Soc.* **63**, 437, 1941; *J. Am. Chem. Soc.* **64**, 1630, 1942.
45. A. Osman and R. Abu-Eittah, *J. Pharm. Sci.* **69**, 1164, 1980.
46. J. Bjerrum, *Metal Amine Formation in Aqueous Solution*, Haase, Copenhagen, 1941.
47. M. Pecar, N. Kujundzic, and J. Pazman, *J. Pharm. Sci.* **66**, 330, 1977; M. Pecar, N. Kujundzic, B. Mlinarevic, D. Cerina, B. Horvat, and M. Veric, *J. Pharm. Sci.* **64**, 970, 1975.
- P.222

48. B. J. Sandmann and H. T. Luk, *J. Pharm. Sci.* **75**, 73, 1986.
49. Y. K. Agrawal, R. Giridhar, and S. K. Menon, *J. Pharm. Sci.* **76**, 903, 1987.
50. K. A. Connors, S.-F. Lin, and A. B. Wong, *J. Pharm. Sci.* **71**, 217, 1982.
51. T. Higuchi and A. A. Zuck, *J. Am. Pharm. Assoc. Sci. Ed.* **42**, 132, 1953.
52. D. Guttman and T. Higuchi, *J. Am. Pharm. Assoc. Sci. Ed.* **46**, 4, 1957.
53. T. Higuchi and J. L. Lach, *J. Am. Pharm. Assoc. Sci. Ed.* **43**, 525, 1954.
54. T. Higuchi and K. A. Connors, in C. N. Reilly (Ed.), *Advances in Analytical Chemistry and Instrumentation*, Vol. 4, Wiley, New York, 1965, pp. 117–212.
55. R. A. Kenley, S. E. Jackson, J. S. Winterle, Y. Shunko, and G. C. Visor, *J. Pharm. Sci.* **75**, 648, 1986.
56. R. Foster (Ed.), *Molecular Complexes*, Vol. 1, Elek, London, 1973.
57. M. A. Slifkin, *Charge Transfer Interactions of Biomolecules*, Academic Press, New York, 1971, Chapters 1 and 2.
58. H. A. Benesi and J. H. Hildebrand, *J. Am. Chem. Soc.* **70**, 2832, 1948.
59. F. A. Al-Obeidi and H. N. Borazan, *J. Pharm. Sci.* **65**, 892, 1976; *J. Pharm. Sci.* **65**, 982, 1976; H. M. Taka, F. A. Al-Obeidi, and H. N. Borazan, *J. Pharm. Sci.* **68**, 631, 1979; N. I. Al-Ani and H. N. Borazan, *J. Pharm. Sci.* **67**, 1381, 1978; H. N. Borazan and Y. H. Ajeena, *J. Pharm. Sci.* **69**, 990, 1980; *J. Pharm. Sci.* **77**, 544, 1988.

60. N. E. Webb and C. C. Thompson, *J. Pharm. Sci.* **67**, 165, 1978.
61. J. Nishijo, I. Yonetami, E. Iwamoto, S. Tokura, and K. Tagahara, *J. Pharm. Sci.* **79**, 14, 1990.
62. H. N. Borazan and S. N. Koumriqian, *J. Pharm. Sci.* **72**, 1450, 1983.
63. J. De Taeye and Th. Zeegers-Huyskens, *J. Pharm. Sci.* **74**, 660, 1985.
64. A. El-Said, E. M. Khairy, and A. Kasem, *J. Pharm. Sci.* **63**, 1453, 1974.
65. A. Goldstein, *Pharmacol. Rev.* **1**, 102, 1949.
66. J. J. Vallner, *J. Pharm. Sci.* **66**, 447, 1977.
67. C. K. Svensson, M. N. Woodruff, and D. Lalka, in W. E. Evans, J. J. Schentag, and W. J. Jusko (Eds.), *Applied Pharmacokinetics*, 2<sup>nd</sup> Ed., Applied Therapeutics, Spokane, Wash., 1986, Chapter 7.
68. G. Scatchard, *Ann. N. Y. Acad. Sci.* **51**, 660, 1949.
69. A. A. Sandberg, H. Rosenthal, S. L. Schneider, and W. R. Slaunwhite, in T. Nakao, G. Pincus, and J. F. Tait (Eds.), *Steroid Dynamics*, Academic Press, New York, 1966, p. 33.
70. J. Blanchard, W. T. Fink, and J. P. Duffy, *J. Pharm. Sci.* **66**, 1470, 1977.
71. I. M. Klotz, F. M. Walker, and R. B. Puvan, *J. Am. Chem. Soc.* **68**, 1486, 1946.
72. T. N. Tozer, J. G. Gambertoglio, D. E. Furst, D. S. Avery, and N. H. G. Holford, *J. Pharm. Sci.* **72**, 1442, 1983.
73. C. J. Briggs, J. W. Hubbard, C. Savage, and D. Smith, *J. Pharm. Sci.* **72**, 918, 1983.
74. A. Zini, J. Barre, G. Defer, J. P. Jeannot, G. Houin, and J. P. Tillement, *J. Pharm. Sci.* **74**, 530, 1984.
75. E. Okezaki, T. Teresaki, M. Nakamura, O. Nagata, H. Kato, and A. Tsuji, *J. Pharm. Sci.* **78**, 504, 1989.
76. J. W. Melten, A. J. Wittebrood, H. J. J. Williams, G. H. Faber, J. Wemer, and D. B. Faber, *J. Pharm. Sci.* **74**, 692, 1985.
77. M. C. Meyer and D. E. Guttman, *J. Pharm. Sci.* **57**, 1627, 1968.
78. J. Judis, *J. Pharm. Sci.* **71**, 1145, 1982.
79. W. Kauzmann, *Adv. Protein Chem.* **14**, 1, 1959.
80. J. B. Nagwekar and H. B. Kostenbauder, *J. Pharm. Sci.* **59**, 751, 1970.
81. H. Kristiansen, M. Nakano, N. I. Nakano, and T. Higuchi, *J. Pharm. Sci.* **59**, 1103, 1970.
82. S. Feldman and M. Gibaldi, *J. Pharm. Sci.* **56**, 370, 1967.
83. M. Menozzi, L. Valentini, E. Vannini, and F. Arcamone, *J. Pharm. Sci.* **73**, 6, 1984.
84. S. Sato, C. D. Ebert, and S. W. Kim, *J. Pharm. Sci.* **72**, 228, 1983.
85. A. M. Saleh, A. R. Ebian, and M. A. Etman, *J. Pharm. Sci.* **75**, 644, 1986.
86. E. Touitou and P. Fisher, *J. Pharm. Sci.* **75**, 384, 1986.
87. E. Touitou, F. Alhaique, P. Fisher, A. Memoli, F. M. Riccieri, and E. Santucci, *J. Pharm. Sci.* **76**, 791, 1987.
88. T. J. Racey, P. Rochon, D. V. C. Awang, and G. A. Neville, *J. Pharm. Sci.* **76**, 314, 1987.
89. J. Coulson and V. J. Smith, *J. Pharm. Sci.* **69**, 799, 1980.
90. F. J. Diana, K. Veronich, and A. Kapoor, *J. Pharm. Sci.* **78**, 195, 1989.
91. J. A. Plaizier-Vercammen, *J. Pharm. Sci.* **72**, 1042, 1983.
92. P. Bustamante and E. Selles, *J. Pharm. Sci.* **75**, 639, 1986.

## Recommended Readings

H. Dodziuk, *Cyclodextrins and Their Complexes: Chemistry, Analytical Methods, Applications*, Wiley-VCH, Weinheim, Germany, 2006.

J. A. Goodrich and J. F. Kugel, *Binding and Kinetics for Molecular Biologists*, Cold Spring Harbor Laboratory Press, New York, 2007.

### Chapter Legacy

**Fifth Edition:** published as Chapter 11 (Complexation and Protein Binding). Updated by Patrick Sinko.

**Sixth Edition:** published as Chapter 9 (Complexation and Protein Binding). Updated by Patrick Sinko.